

THESIS FOR THE DEGREE OF DOCTOR OF PHILOSOPHY

Absorption Based Systems for Co-removal of Nitrogen
Oxides and Sulfur Oxides from Flue Gases

JAKOB JOHANSSON

Department of Space, Earth and Environment
Division of Energy Technology
CHALMERS UNIVERSITY OF TECHNOLOGY

Gothenburg, Sweden 2022

Absorption Based Systems for Co-removal of Nitrogen Oxides and Sulfur
Oxides from Flue Gases
JAKOB JOHANSSON
ISBN 978-91-7905-701-5

© JAKOB JOHANSSON, 2022.

Doktorsavhandlingar vid Chalmers tekniska högskola
Ny serie nr 5167
ISSN 0346-718X

Department of Space, Earth and Environment
Division of Energy Technology
Chalmers University of Technology
SE-412 96 Gothenburg
Sweden
Telephone + 46 (0)31-772 1000

Printed by Chalmers Reproservice
Chalmers University of Technology
Gothenburg, Sweden 2022

Absorption Based Systems for Co-removal of Nitrogen Oxides and Sulfur
Oxides from Flue Gases
JAKOB JOHANSSON
Department of Space, Earth and Environment
Division of Energy Technology
Chalmers University of Technology

Abstract

Enhanced control of nitrogen and sulfur emissions, found in many of industrial processes, is anticipated for decades to come. Stricter emission regulations require new technologies adapted to the new conditions at reasonable cost. Multi-pollution control is an efficient way to lower costs, although difficult to implement, and the co-removal of NO_x and SO_x is therefore presently achieving much attention.

This thesis covers five studies that are focused on the concept of co-removal of NO_x and SO_x in a wet scrubber unit, whereby the NO is oxidized to NO_2 by the introduction of a gaseous oxidizing agent, ClO_2 , into the flue gas stream before the scrubber. The gas phase oxidation of NO to NO_2 by ClO_2 has been tested for a wide variety of flue gas compositions and temperatures, applying a total of three intermediate scales: 0.2 Nm^3/h with synthetic flue gases, 100 Nm^3/h with flue gases from a propane flame, and a ~ 400 Nm^3/h slip stream from a waste-to-heat plant. An efficient NO to NO_2 oxidation was observed at all scales with complete conversion at a ClO_2/NO ratio of ~ 0.5 . No interaction between ClO_2 and SO_2 or other flue gas impurities was observed, which is important to minimize ClO_2 consumption.

In terms of the absorption process, a number of liquid compositions has been tested in four setups, showing that the concentrations of SO_2 and NO_2 in the flue gas can both be reduced to a few ppm. The rate of NO_2 removal is strongly dependent upon the presence of SO_3^{2-} and HSO_3^- in the absorbing liquid. To study this interaction a new method for on-line analysis of the liquid composition in the system is developed. The SO_3^{2-} and HSO_3^- oxidation caused by NO_2 absorption and O_2 is investigated and concluded to be following a radical initiated chain. It is also confirmed that this chain is efficiently interrupted by $\text{S}_2\text{O}_3^{2-}$. The derived model gives good agreement with the experimental outcomes for the 100 Nm^3/h and 400 Nm^3/h setups. A design for full scale implementation at a 20 MW_{th} waste-to-heat plant is proposed together with cost estimation for installation and operation. The work of this thesis represents the first validation of the concept and methodology of scale-up of the co-removal process and paves the way for commercialization.

Keywords: Emissions control, NO_x , SO_x , ClO_2 , absorption, scale-up, gas-phase oxidation, sulfite oxidation

List of Publications

This thesis is based on the following papers, which are referred to in this thesis according to their Roman numerals:

- I. Johansson, J.; Hulten, A. H.; Ajdari, S.; Nilsson, P.; Samuelsson, M.; Normann, F.; Andersson, K., *Gas-Phase Chemistry of the NO-SO₂-ClO₂ System Applied to Flue Gas Cleaning*. Industrial & Engineering Chemistry Research 2018, 57, (43), 14347-14354.
- II. Johansson, J.; Normann, F.; Sarajlic, N.; Andersson, K., *Technical-scale Evaluation of Scrubber-based, Co-Removal of NO_x and SO_x Species from Flue Gases via Gas-Phase Oxidation*. Industrial & Engineering Chemistry Research 2019, 58, (48), 21904-21912.
- III. Johansson, J.; Hulten, A. H.; Normann, F.; Andersson, K., *Simultaneous Removal of NO_x and SO_x from Flue Gases Using ClO₂: Process Scaling and Modeling Simulations*. Industrial & Engineering Chemistry Research 2021, 60, (4), 1774-1783.
- IV. Johansson, J.; Normann, F.; Andersson, K., *Techno-Economic Evaluation of Co-Removal of NO_x and SO_x Species from Flue Gases via enhanced oxidation of NO by ClO₂ - Case Studies of Implementation at a Pulp and Paper Mill, Waste-to-Heat Plant and a Cruise Ship*. Energies 2021, 14, 8512.
- V. Johansson, J.; Wagaarachchige, J. D.; Normann, F.; Jens, K. J.; Andersson, K., *The Influence of Nitrogen Dioxide Absorption on Sulfite Oxidation Rate in the presence of Oxygen: On-Line Raman Measurements*. To be submitted.

In addition, the following paper is included in the Appendix:

- A. Gall, D.; Allgurén, T.; Johansson, J.; Normann, F.; Hulten, A. H.; Gunnarsson, A.; Andersson, K., *Recirculation of NO_x and SO_x scrubber effluent to an industrial grate fired MSW boiler – influence on combustion performance, deposition behavior and flue gas composition*. Energy Fuels 2022, 36, (11), 5868-5877.

Jakob Johansson, who is the main author of all five papers, was responsible for the experimental work in **Paper I-IV** and data evaluation in all the papers, as well as for the modeling work in **Paper II-IV**. Professor Fredrik Normann and Professor Klas Andersson contributed with discussions and editing for all the papers. Dr. Sima Ajdari conducted the NO₂-SO₂ experiments and modeling in **Paper I**. Nadine Sarajlic contributed to the modeling in **Paper II**. Dr. Anette Heijnesson-Hultén, Pär Nilsson and Marie Samuelsson took part in the experiments described in **Paper I**. Dr. Anette Heijnesson-Hultén also contributed to the experiments described in **Paper III**, as well as to the editing of the paper. Jayangi Dinesha Wagaarachchige, and Professor Klaus Joachim Jens was responsible for execution of experiments and construction of Raman model in **Paper V**.

Acknowledgments

I would like to express my gratitude to Nouryon, Nordic Energy Research and Energimyndigheten for supporting this work financially. Special thanks to the team at Nouryon, who have played a vital role in this work since day one.

A large thank you to my supervisor, Klas Andersson for the guidance and inspiration that you have given me and for offering me this position.

I would like to express my appreciation to the research engineers at Chalmers Kraftcentral – you have all assisted me in one way or another – and a special thanks to Johannes Öhlin who has been there during the experiments, teaching me and keeping things in order, always with a smile. Thanks to the A-Team for helping with everything.

Adrian Gunnarsson, Thomas Allgurén, Daniel Bäckström and Dan Gall, I hope that I atleast have given you something, because you have given me a lot. Experiments are never dull, but they are pure fire when you are participating.

To all my colleagues at Energy Technology, you are a big part of why I applied for this position. This working place is truly fantastic in having so many great colleagues.

Fredrik Normann, you have been there for me throughout this whole time. I have learnt so much from you and I hope that in this process, you have learnt something from me aswell. You are a source of inspiration and information, and your door is always open, for which you have my deepest thanks.

Finally, I want to thank all those persons outside Chalmers who mean the world to me. My fantastic friends, my wonderful parents and brother and the most precious thing I have in life, my family. Julia och Bosse, jag älskar er.

Jakob Johansson
Gothenburg, Sweden, 2022

Table of Contents

Abstract	I
List of Publications	III
Acknowledgments	V
1 Introduction	1
1.1 Aim of Research.....	2
1.2 Outline of the Thesis	4
2 Methodology	5
2.1 Data Evaluation	7
2.2 Experimental Setups.....	8
2.3 Modeling	17
3 Conventional Flue Gas Treatment	21
4 Previous Work and Progress Made	23
4.1 Oxidation of NO to NO ₂	23
4.2 Combined Absorption of NO ₂ and SO ₂	28
4.3 Sulfite Oxidation	30
5 Chemistry	33
6 Selected Results and Discussion	37
6.1 Validation of the Enhanced Oxidation of NO	37
6.2 Simultaneous Absorption of NO _x and SO _x	41
6.3 Validation of the Reaction Mechanism	45
6.4 Modeling of Continuous Operation.....	47
6.5 On-line monitoring of sulfite oxidation	49
7 Conclusions	53
8 Suggestions for Future Work	55
Bibliography	57

CHAPTER 1

Introduction

Air pollution is a serious environmental issue with direct effect on human health. Almost the entire global population (>99%) breath air that exceeds the World Health Organization (WHO) guideline limits. Particulate matter (PM), ground-level ozone, nitrogen oxides (NO_x), and sulfur oxides (SO_x) are considered the four main constituents of air pollution. All of these are products, directly or indirectly, of combustion.¹ For the effect of any of these emissions to be acute, the concentrations need to be high, often higher than what can be accumulated in a ventilated area. Instead, the danger lies in long-term exposure.² The WHO estimates that 7.6% of all deaths worldwide in 2016 were related to the above mentioned ambient air pollution.

Since primary energy sources harnested through combustion represent a simple and low-cost access to energy with an established infrastructure, it is likely that combustion will remain a vital part of our energy supply for a long time. Figure 1 shows the distribution in global primary energy supply from 1990 to 2019. In 2019, around 10% of the global primary energy supply originated from sources that are considered “free” of direct ambient air pollutants (hydroelectricity, nuclear energy and renewables, excluding biomass). Even though wind and solar power generation is increasing rapidly, it is currently outpaced by the increase in energy consumption. These trends and the order of magnitude of combustion motivate exploration of the potential of flue gas cleaning, not only in terms of its application today but also its value for generations to come. This work focuses on the reduction of NO_x and SO_x in gaseous emissions.

Emissions of NO_x have been established as a source of ozone, smog and acid rain formation. Smog or ‘smoky fog’ may form from emissions in populated areas. The original type of smog, which was more common before 1960 but remains a problem in some parts of the world, was formed from direct emissions originating from incomplete combustion, most commonly of coal. This type of smog is especially common during winter inversions when emissions levels are higher and tend to accumulate at ground level. The type of smog that is more commonly observed today, known as photochemical smog, involves chemical reactions between NO_x and hydrocarbons in the atmosphere and is enhanced by radiation from the sun, forming a number of harmful chemicals. Photochemical smog is a major problem in many large cities around the world, such as Beijing, Los Angeles and Mexico City.

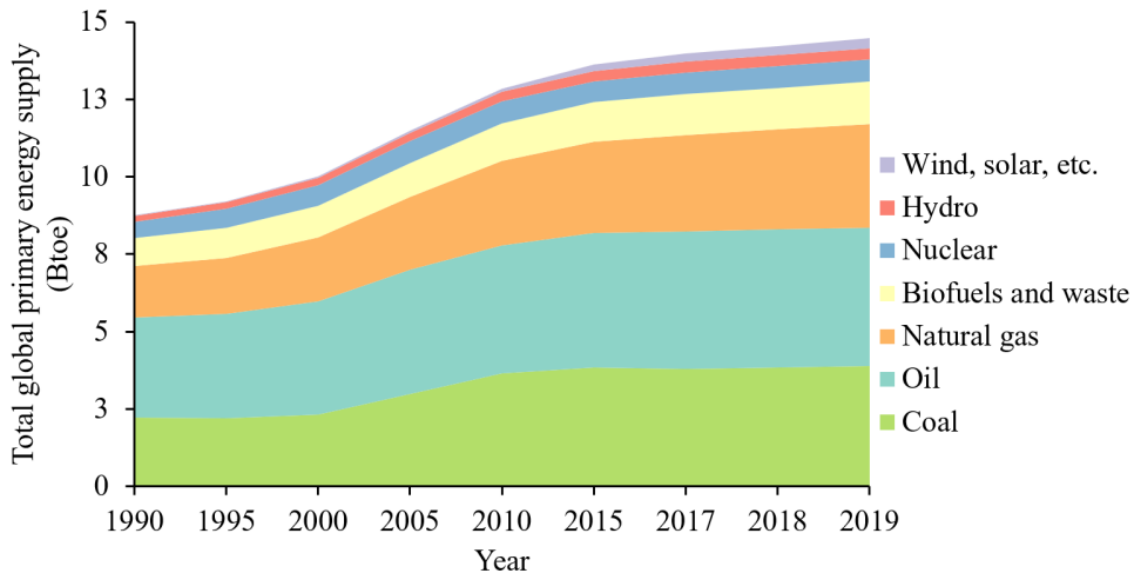


Figure 1: Total global primary energy supply divided by source, from 1990 to 2019 in billion tonne of oil equivalents (Btoe). Data from the IEA Policies and Measures Database © OECD/IEA.³

Acid rain, while not directly harmful to humans, is still a concern in many places around the world. Acid rain refers to rain that has an increased number of hydrogen ions, produced from reactions with SO_x and NO_x . Acid rain can, as such, have a direct impact on the pH levels of lakes and other wetlands. Many plants and even animals are not adapted to changes in pH, and acid rain is the reason for extinction of life in many lakes. In cities, acid rain causes corrosion and deterioration of structures, especially those made of marble or limestone, as these materials are rich in calcium that reacts with the acids.

Since the downside of emitting SO_x and NO_x is well-established, regulations have for several decades pushed for the development of reduction technologies. Currently, it is possible to remove sulfur from liquid and gaseous fuels before combustion, reduce the amount of NO_x formed during combustion, and capture the SO_x and NO_x from the flue gases. These technologies may, however, not be optimal for all types of emissions sources. As the regulations start to affect a wide variety of industries and end-users, new and tailored technologies are needed to maintain competitiveness.

1.1 Aim of Research

A flue gas cleaning concept that is gaining momentum is to absorb NO_x and SO_x simultaneously in one and the same unit. Figure 2 shows an overview to the concept. This thesis investigates the specific application where ClO_2 is used as an oxidizing agent to oxidize NO to NO_2 in a fast gas phase reaction followed by a wet absorption unit where NO_2 and SO_2 is removed as liquid phase products.

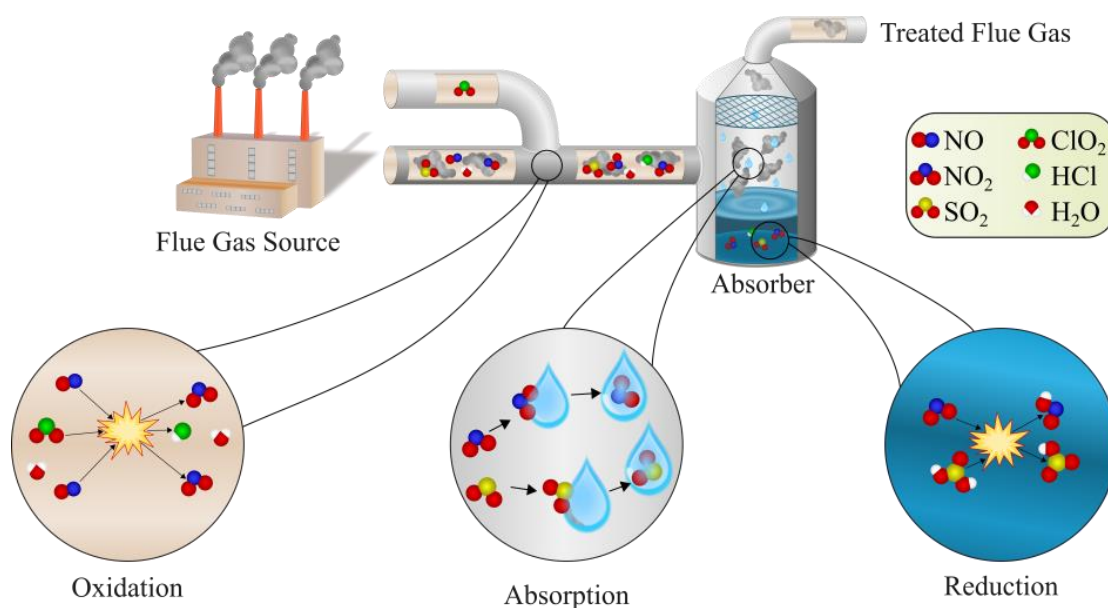


Figure 2: Overview of the investigated concept for simultaneous removal of NO_x and SO_x from flue gases in a process that employs enhanced oxidation of NO by ClO_2 .

While this work focuses specifically on a process based on enhanced oxidation of NO by ClO_2 , the liquid phase chemistry investigated is applicable for a wide variety of processes. The work combines experimental studies with modeling. The experimental studies aim to develop and demonstrate process performance. The modeling aims to interpret the chemistry active during the experiments, and to predict the performance of the final concept in different applications. More specifically the thesis aims to contribute to the process development in four main areas:

- **NO oxidation:** The efficiency of ClO_2 as an oxidizing agent for gas-phase oxidation of NO to NO_2 .
- **Absorption:** The performance of the liquid-phase chemistry in a combined SO_x - NO_x scrubbing system.
- **Sulfite oxidation:** The rate of liquid phase sulfite oxidation and development of online measurement techniques for continuous measurement.
- **Technology:** Process design and optimization of supporting chemicals.

Furthermore, the thesis develops a method for efficient verification and up-scaling of the technology including several measurement setups and a modelling procedure.

1.2 Outline of the Thesis

The thesis consists of an introductory essay and five appended papers. The introductory essay places the work in the context of current knowledge, introduces the main theory behind the proposed concept, and describes the methodology. The essay concludes with the key findings from the work and proposes a way forward. The thesis is based on the five appended papers, which are summarized below.

Paper I is an experimental investigation of the gas-phase interactions between NO, SO₂ and ClO₂.

Paper II is an experimental investigation of the simultaneous absorption of SO_x and NO_x at technical scale. **Paper II** also describes the first validation of the previously proposed state-of-the-art reaction mechanism of the liquid-phase chemistry of a SO_x/NO_x scrubber system.

Paper III compares the performances of three scales of the co-removal system used in the work and discusses the up-scaling of the concept. This paper includes experimental results, as well as the outcomes of the process modeling.

Paper IV is a techno-economic analysis of full scale implementation of the SO_x/NO_x treatment system for three flue gas sources: a medium sized waste-to-heat plant; the kraft recovery boiler of a pulp and paper mill; and a cruise ship.

Paper V is an experimental investigation of the liquid phase oxidation of SO₃²⁻ and HSO₃⁻ caused by absorbed NO₂ and O₂.

CHAPTER 2

Methodology

The performance of the concept is evaluated experimentally in steps based on a number of key performance indicators (discussed in the next section), following up-scaling of the process. Figure 3 pictures the overall methodology of the up-scaling and investigation of process chemistry.

The concept was first evaluated in a bench-scale unit, treating 0.2 Nm³/h of a simulated flue gas flow. Initially, the efficiency of ClO₂ as an oxidizing agent for gas-phase oxidation of NO to NO₂ was established for a wide variety of flue gas temperatures and compositions (**Paper I**). The remainder of the work focused on the efficiency and the implementation of the absorption process. The effects of the pH level, temperature and additives of the absorbing liquid, as well as the flue gas composition formed the main focus.

For the technical-scale testing, the 100-kW oxy-fuel unit at Chalmers was retrofitted with the required flue gas cleaning path. At 100 Nm³/h, many of the issues related to small-scale scrubbing at 0.2 Nm³/h are avoided and the technical feasibility may be evaluated. The 100 Nm³/h unit was used to test the concept for a combustion-derived flue gas, with scrubbing in a purpose-built scrubber and with consideration of safety issues related to the used chemicals. The experimental results represent a first dataset for validation of the reaction mechanism previously proposed by our research group (Ajdari et. al⁴) (**Paper II**).

The 400 Nm³/h field-testing unit is capable of evaluating the concept at different sites and in a continuous mode of operation. The scrubber unit has a design similar to that of the 100 Nm³/h unit but offers an automated process control with continuous flows and more measurement points. For these tests, the unit was installed at a waste-to-heat plant where a slipstream of the flue gas was led to the field-testing unit. The 400 Nm³/h unit allowed the acquisition of new expertise regarding the implementation of the process and process control. **Paper III** summarizes and compares the performance of the process across the scales tested leading to a discussion of the up-scaling methodology.

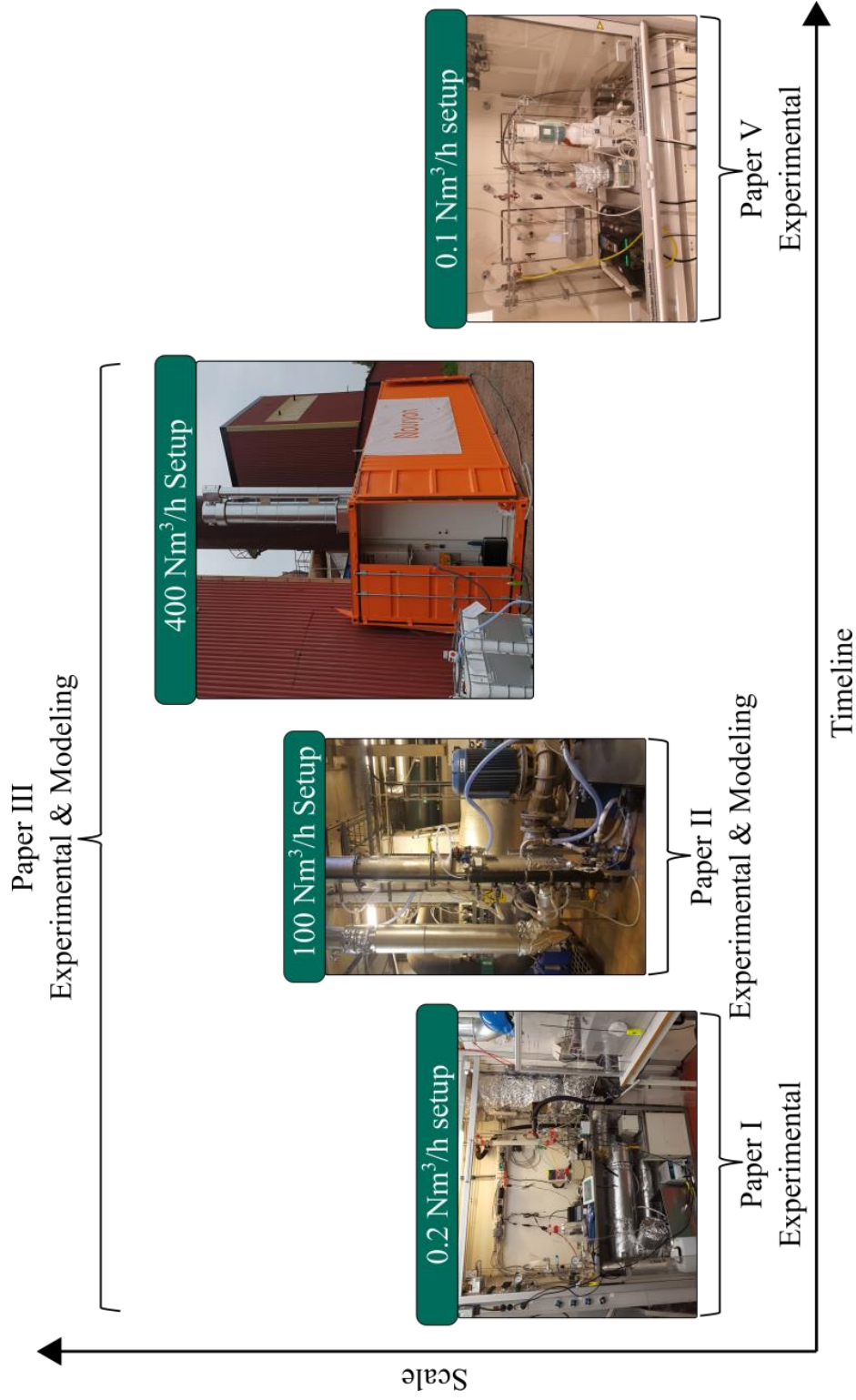


Figure 3: Relationship between Papers I to III and V and the five experimental setups that constitute the basis for the thesis. Left: 0.2 Nm³/h setup used for gas phase oxidation and simultaneous absorption experiments, Middle left: The oxidation reactor and scrubber of the 100 Nm³/h setup attached to Chalmers 100 kW oxy-fuel combustor, Middle right: The 12 m long container housing the 400 Nm³/h setup attached with a slip stream from the WTHP Källhagsverken in Avesta and Right: 0.1 Nm³/h setup used for sulfite oxidation experiments.

With the large amount of knowledge gathered from the three experimental setups, a techno-economic study was performed (**Paper IV**) where combined NO₂-SO₂ removal was evaluated for three flue gas sources; a medium-sized waste-to-heat plant (20 megawatt thermal, MW_{th}); a medium-sized pulp and paper mill (500,000 tons pulp/year) recovery boiler; and a cruise ship (12 MW). The technical performance of each case was investigated through simulations based on previous experimental results. Economic evaluations were then performed based on the technical study. Each application has important differences in operating conditions and in emission standards why the technological and economic performance will vary between cases.

The final contribution of this thesis is a study of the liquid phase chemistry related to combined NO₂-SO₂ removal (**Paper V**). Of specific interest is the oxidation of S(IV) (SO₃²⁻ and HSO₃⁻) to S(VI), (SO₄²⁻) caused by NO₂ absorption. The concentration of S(IV) is the single most important parameter for NO₂ absorption. The reaction between NO₂ and S(IV) and subsequent reactions are difficult to analyze due to high reaction rates and extractive analysis methods risk to miss the entire course of reactions and only provide quantification of end products. To enable on-line measurements of the reaction course in a combined NO₂-SO₂ removal system, an analysis method in Raman spectroscopy was developed and tested in a lab-scale setup with simulated flue gases.

2.1 Data Evaluation

The evaluation of the results is based on a few key performance indicators, as defined below. The molar ratio between added ClO₂ and the NO after combustion to be oxidized is defined as:

$$r_{\text{ClO}_2} = \frac{\text{ClO}_2}{\text{NO}_{\text{pre-oxidation}}}. \quad (2.1)$$

The performance of the NO oxidation process is indicated by the NO conversion, which is based on the measured dry concentration of NO before and after the oxidation reactor:

$$\text{NO conversion} = 1 - \frac{\text{NO}_{\text{post-oxidation}}}{\text{NO}_{\text{pre-oxidation}}}. \quad (2.2)$$

The amount of NO_x absorption is defined as the rate of reduction of NO_x in the flue gas, which is based on the measured dry concentrations of NO and NO₂ before the oxidation reactor and after the scrubber:

$$\text{NO}_x \text{ absorption} = 1 - \frac{\text{NO}_{\text{post-scrubber}} + \text{NO}_{2,\text{post-scrubber}}}{\text{NO}_{\text{pre-oxidation}} + \text{NO}_{2,\text{pre-oxidation}}}. \quad (2.3)$$

Note that the total amount of NO and NO₂ after the oxidation reactor may be slightly lower than before the reactor due to losses in the pipes, why the NO_x measured before the oxidation reactor is used to evaluate NO_x absorption.

When the specific absorption of NO₂ or NO is evaluated, the dry-basis concentrations before and after the scrubber are used as follows:

$$\text{NO}_2 \text{ absorption} = 1 - \frac{\text{NO}_{2,\text{post-scrubber}}}{\text{NO}_{2,\text{post-oxidation}}}, \quad (2.4)$$

$$\text{NO absorption} = 1 - \frac{\text{NO}_{\text{post-scrubber}}}{\text{NO}_{\text{post-oxidation}}}. \quad (2.5)$$

Similar to NO conversion, SO₂ conversion is defined as follows:

$$\text{SO}_2 \text{ conversion} = 1 - \frac{\text{SO}_{2,\text{post-oxidation}}}{\text{SO}_{2,\text{pre-oxidation}}}. \quad (2.6)$$

The absorption of SO₂ is equally important as the absorption of NO₂ and is defined similarly to NO₂ absorption as:

$$\text{SO}_2 \text{ absorpotion} = 1 - \frac{\text{SO}_{2,\text{post-scrubber}}}{\text{SO}_{2,\text{post-oxidation}}}.$$

The relation between S(IV) in the absorption liquid and NO₂ in the gas phase is an important parameter for absorption efficiency. The ratio between these two is defined as:

$$\text{S(IV)} / \text{NO}_2 = \frac{\text{SO}_{2,\text{absorbed}} + \text{Na}_2\text{SO}_{3,\text{added}}}{\text{NO}_{2,\text{pre-scrubber}}}.$$

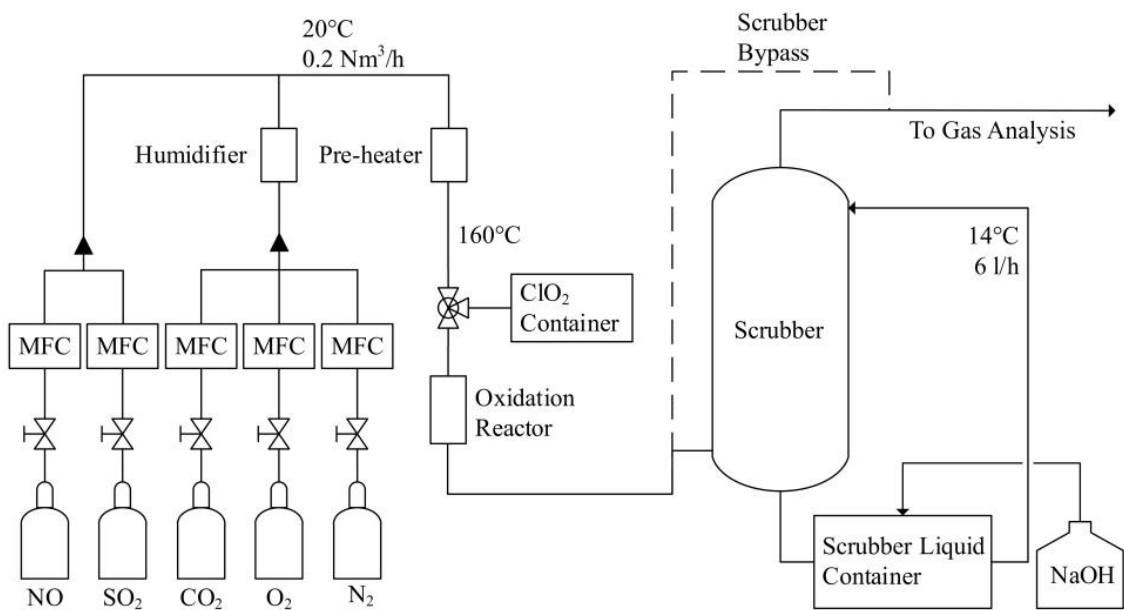
2.2 Experimental Setups

2.2.1 The 0.2 Nm³/h Unit

The 0.2 Nm³/h unit is outlined in Figure 4. The desired gas compositions are obtained through the mixing of N₂, CO₂, O₂, NO, and SO₂. Water is added in a humidifier. The ClO₂ gas is added to the gas mixture under various process conditions. The flue gas compositions and process conditions used in this study are presented in Table 1.

Table 1: Investigated parameters and their set values, as used in the 0.2 Nm³/h unit.

Parameter	Value
Inlet SO ₂ concentration	400 ppm
Inlet NO concentration	200 ppm
Inlet O ₂ concentration	3%
Inlet CO ₂ concentration	10%
Humidifier H ₂ O levels	0%, 10%, 15%, 25%
Inlet N ₂ concentration	Balance
Reactor temperature	160°C
r _{ClO₂}	0.2, 0.4, 0.6

**Figure 4:** Process outline of the 0.2 Nm³/h unit. The black line is the gas flow, the solid line indicates the major route, and the dashed line represents a bypass of the scrubber. MFC, Mass flow controller.

The gases used in the gas mixing system are: N₂ (100%), CO₂ (100%), O₂ (100%), SO₂ (10% in N₂), and NO (10% in N₂) (all from AGA Linde). The addition of the gases is controlled using Bronkhorst mass flow controllers (MFCs; EL-Flow series). Water vapor is produced by the Bronkhorst controlled evaporation and mixing (CEM) system supplied by Omni Process, Sweden. The water vapor is added to the flue gas stream in close conjunction with the pre-heater, in order to avoid condensation. The pre-heater (made of stainless steel) and reactor system (made of titanium) consists of two pipes that are heated with oil. The pipes are connected by a mixing zone where the ClO₂ gas is added. This system provides a uniform reaction temperature ($\pm 1^\circ\text{C}$) up to a temperature of 300°C. The ClO₂ gas is produced from an aqueous chlorine

dioxide solution (ClO_2 gas dissolved in water) by stripping. Nitrogen is allowed to pass through a bubble plate into a flask, thereby releasing ClO_2 gas. The charge of ClO_2 gas is controlled by choosing an appropriate nitrogen flow through an aqueous ClO_2 solution of known concentration at a specified temperature. The temperature is maintained by a water-bath, and the concentration of the solution is continuously determined by circulating the aqueous chlorine dioxide through a spectrophotometer (Hach Lange DR 2800).

After the oxidation reactor, the flue gas enters a scrubber (Günter DIEHM Process Systems, Germany), which is random-packed with Raschig rings measuring 6×6 mm, composed of borosilicate glass, and operating with a counter-flow liquid stream. The absorption solution was recirculated during the trial and the pH level was varied from 1 to 10 by adding 1 M hydrochloric acid (HCl, laboratory grade) or 1 M sodium hydroxide (NaOH, Scharlau, laboratory grade). The flue gas is led via Teflon-lined heated tubes to the Fourier-transform infrared spectroscopy (FTIR) gas analyzer. The gas can also bypass the scrubber, allowing determination of the gas composition after the oxidation reactor. The FTIR is the MKS MultiGas™ 2030, which is capable of measuring NO, NO_2 , HNO_3 , N_2O , SO_2 and HCl, as well as other less-likely species for the system. Gases of interest that are not measured by the FTIR include Cl_2 and O_2 , which are not active in the IR spectrum, as well as HNO_2 .

2.2.2 The 100 Nm^3/h Unit

The 100 Nm^3/h unit is outlined in Figure 5. The setup consists of six main parts: the furnace, flue gas cooler, oxidation reactor, ClO_2 generator, scrubber, and scrubber liquid storage and distribution system. Apart from the furnace, which has been described in detail by Andersson et al.,⁵ all the parts were designed and constructed for the present investigation. The flue gas cooler was redesigned to facilitate control of the exiting gas temperature within the range of $100^\circ\text{--}400^\circ\text{C}$. The ClO_2 used to oxidize NO to NO_2 is generated in an electrolytic cell from NaClO_2 and H_2O using a generator (CDE10; Dioxide Pacific). The generated ClO_2 is diluted with ambient air (up to 3% ClO_2) and injected into the flue gas path through a perforated pipe, which is composed of stainless steel. Immediately after the mixing of the two streams, the flue gas path is widened to function as a reactor in which the oxidation takes place.

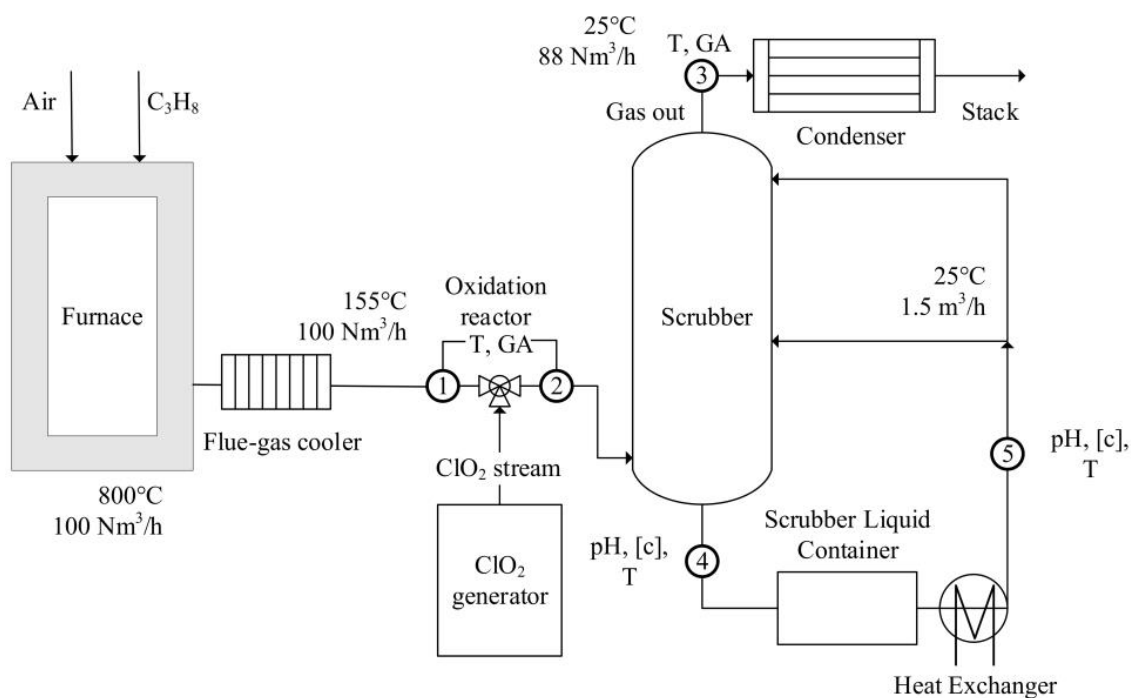


Figure 5: Process outline of the 100 Nm³/h setup. Circles indicate the measurement locations. T, temperature; GA, gas analyzer; pH, scrubber liquid pH level; and [c], scrubber liquid compositions in terms of N(III), N(V) and S(VI).

The diameter of the pipe is expanded via a 200-mm-long cone from 100 mm to 200 mm. The residence time in the reactor is approximately 1 second under standard operating conditions. The flue gas path and the reactor are constructed of stainless steel (SS2343). After the oxidation reactor, the flue gas enters the scrubber. The scrubber is divided into two sections: a bottom section of height 2.6 m, and a top section of height 1.8 m. The bottom section is a spray tower scrubber with three vertically, evenly distributed inlets fitted with screw nozzles (BETE TF, Hansa Engineering). The bottom section of the scrubber has a diameter of 260 mm and the liquid exits through a drainage port at the very bottom of the reactor. The upper part of the scrubber can be toggled between a spray tower configuration (same specifications as the bottom section and with drainage between the two sections) and a packed bed configuration with diameter of 300 mm and packed height of 2 m.

The packing material used has a metal saddle construction, with a specific surface area of 100 m²/m³. The packed bed configuration is supplied with liquid through a screw nozzle at the top. In this configuration, all the liquid exits via the bottom drainage port. The scrubber liquids from the two sections are collected in a tank, in which the pH level is adjusted (based on the pH of the scrubber liquid being fed to the scrubber) by the addition of NaOH (50 wt.%). The scrubber liquid is maintained at 25°C. An installed pump connects to the scrubber liquid feedline and can be used to introduce additives, if so desired.

The gas-phase composition and temperature are measured at three positions in the system (Positions 1, 2, and 3 in Figure 5): before and after the addition of ClO₂ (to establish the rate of oxidation of NO to NO₂), and after the scrubber (to determine the removal efficiency). The flue gas is extracted via Teflon-lined pipes heated to 160°C, and the gas composition is measured in the MultiGas 2030 FTIR Continuous Gas Analyzer. The scrubber liquid can be extracted from the bottom tank, after the pump, as well as from the top and bottom drainage ports. The liquid compositions in the bottom tank and after the pump (what is fed to the scrubber) would ideally be identical assuming perfect mixing. However, there is no forced mixing of the bottom tank. The compositions in terms of N(III), N(V) and S(VI) are measured by ion chromatography. The concentrations of S(IV) in the absorbing liquids of the experiments are difficult to assess since S(IV) oxidizes in the presence of O₂.

The experiments assayed a variety of flue gas compositions and scrubber liquids, as specified in Table 2. As the pH of the scrubber liquid is believed to have a significant impact on the absorption, four pH levels were tested: 1, 5, 7 and 9.⁶ As the partial pressure of a gas in an absorption process affects the solubility, according to Henry's law, different gas concentrations of NO_x and SO_x were tested. The presence of SO₂ has also been shown to enhance the absorption of NO₂ through an interaction between S(IV) and N(III). Na₂SO₃ is added directly to the scrubber liquid to increase the rate of this interaction, and Na₂CO₃ is added as a buffer to prevent a pH drop. Some experiments were also performed with a decreased flue gas flow (denoted as “reduced flow”), to investigate the effect of increased gas residence time in the scrubber. The flue gas flow in these experiments was 60 Nm³/h.

Table 2: Process parameters evaluated in the 100 Nm³/h unit, including the wet gas concentrations from the combustion (Position 1 in Figure 5), the ClO₂ added to the oxidation reactor (Position 2), and the scrubber liquid composition (Position 5).

Species	Low limit	High limit
Flue gas composition		
SO ₂ (ppm)	0	500
NO (ppm)	70	350
O ₂ (vol%)	2.9	7.3
Added oxidizing agent		
r _{ClO₂} (mol _{ClO₂} /mol _{NO})	0.2	0.4
Scrubber liquid additive		
Na ₂ SO ₃ (g/l)	0	1
Na ₂ CO ₃ (wt.%)	0	10

2.2.3 The 400 Nm³/h Unit

The 400 Nm³/h unit is outlined in Figure 6. The setup, with the exception of the scrubber, is enclosed in a 12-meter-long container. Thus, it is a mobile unit that is suitable for field testing at industrial sites. The discussed test was performed at the Källhagsverken plant in Avesta, Sweden. Källhagsverken is a grate-fired waste incineration plant, producing heat for the city of Avesta. The flue gas composition varies with time, owing to variations in the fuel. The 72-hour mean values for the compositions with standard deviations are presented in Table 3. A slipstream is taken from the main flue gas line after the existing NO_x control (selective non-catalytic reduction, SNCR) and PM control (electrostatic precipitator, ESP). The flue gas is transported via insulated steel pipes to the container, where it is connected to Teflon-lined pipes. ClO₂ is injected into the gas stream, and the flue gas composition is analyzed again 8-meters downstream, after which it is fed to a quench. The quench is meant to remove all Cl-containing compounds, to avoid carry-over to the scrubber, so as to prevent corrosion of the equipment and minimize water loss/accumulation in the scrubber as well as to cool the flue gas before the scrubber due to material constraints. The flue gas leaves the quench saturated with water. The scrubber is not cooled and operates at the saturation temperature corresponding to the water content from combustion. The scrubber tower is packed with pall rings (25 mm) and is 4.8 meters in height. The flue gas is transported via a fan back to the main flue gas stream of the plant.

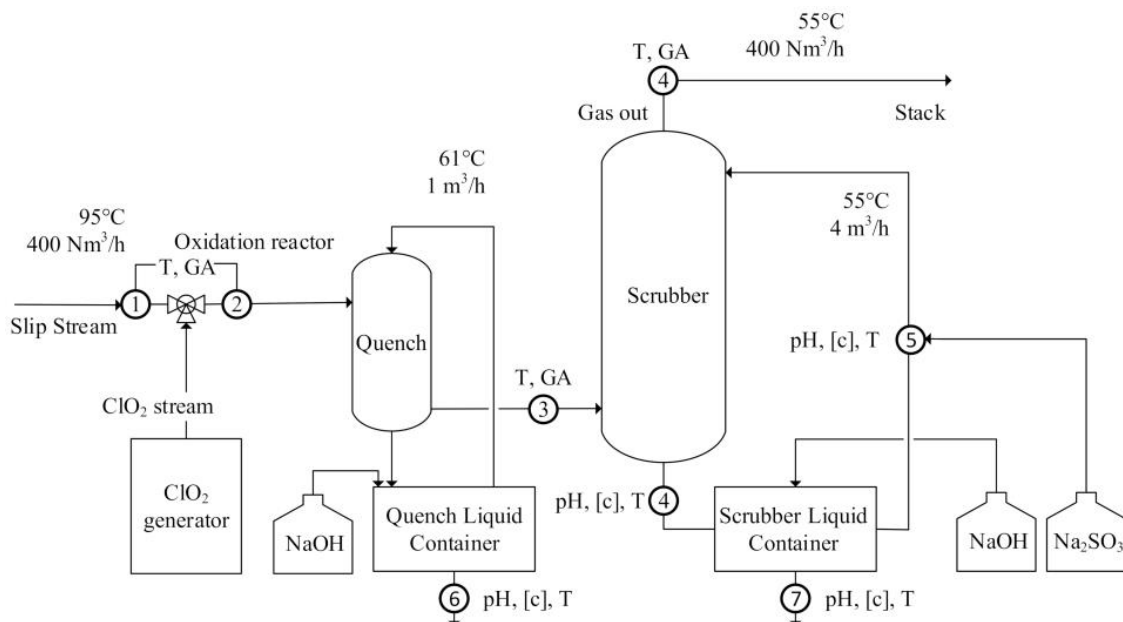


Figure 6: Process outline of the 400 Nm³/h unit. Circles indicate measurement locations. T, temperature; GA, gas analyzer; pH, pH level; and [c], liquid concentrations.

Table 3: Flue gas composition for the 400 Nm³/h unit. Shown are the 3-day averages, with standard deviation in parentheses.

Parameter	400 Nm ³ /h setup
N ₂ (%)	Balance
CO ₂ (%)	9.9 (1)
H ₂ O (%)	14.7 (2)
O ₂ (%)	5.8 (0.9)
SO ₂ (ppm dry)	233 (127)
NO (ppm dry)	72 (20)
CO (ppm dry)	34 (34)

The conditions used for application to a commercial plant differ from those in the controlled experiments, as the process control must consider transient flue gas concentration. The dosing of ClO₂ to the flue gas stream is adjusted in 20-minute intervals based on the average measured NO concentration for the previous two 10-minute periods. This level of control is slow compared to the fluctuations in inlet NO concentration. The ClO₂ feed is set at 20% above the theoretical value for oxidizing the mean NO value ($r_{\text{ClO}_2}=0.48$), to balance NO oxidation and ClO₂ consumption.

The 400 Nm³/h unit and the waste-to-heat plant Källhagsverket in Avesta has also been used for research regarding the wastewater treatment of the NO_x-SO_x removal process. The scrubber effluent of the 400 Nm³/h unit was gathered during operation to investigate if recirculation of the liquid to the grate-fired boiler of the waste-to-heat plant could facilitate an efficient way of wastewater treatment. The liquid contains high concentrations of S(VI) and N(III) and thermal treatment of these species could result in reduction of N(III) to N₂ and S(VI) to SO₂. A schematic of the 20 MW_{th} waste to heat plant including the proposed design of a recirculation stream from the scrubber is displayed in Figure 7. The combustion characteristics were carefully studied during the injections to observe the potential effects on burnout and flue gas composition. In addition, deposition measurements were performed to observe effects on growth rate and chemical composition of deposits, which are critical factors for any solid fuel-fired heat and power plant. This research is described in greater detail in the Paper A included in the appendix of this thesis.

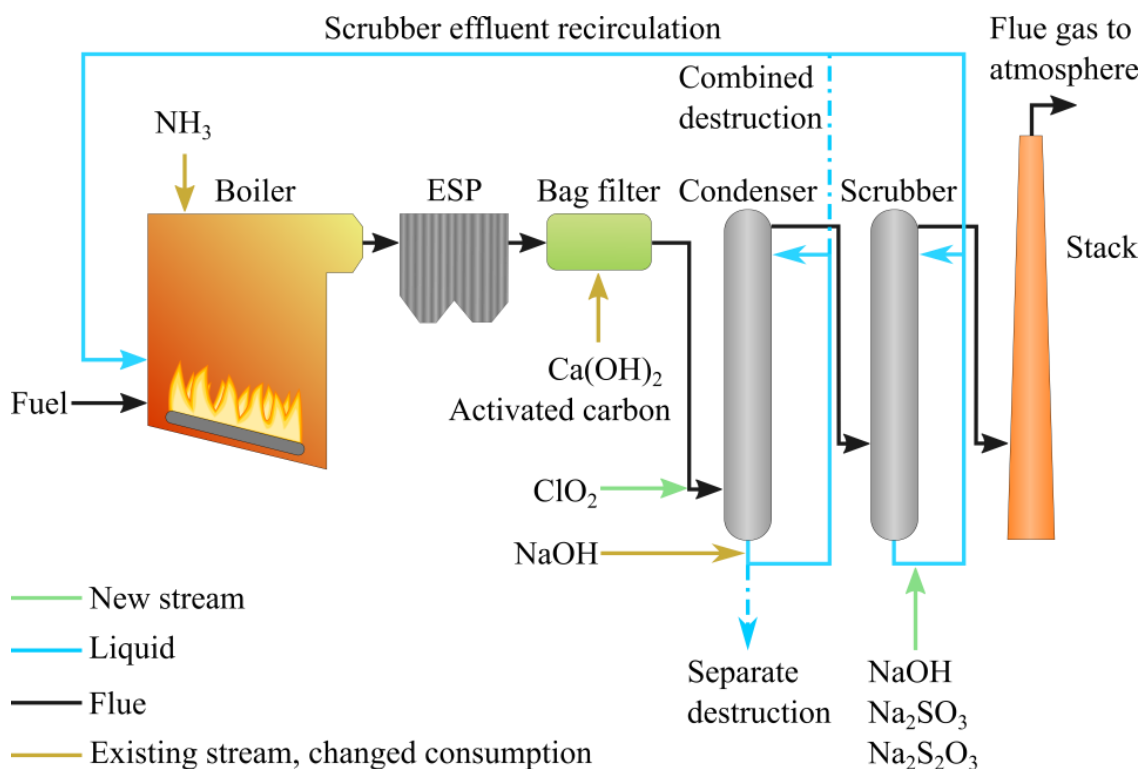


Figure 7: Schematic of the 20 MW_{th} waste-to-heat plant, including the recirculation streams from the scrubber and condenser as a proposed design.

2.2.4 The 0.1 Nm³/h Raman Unit

Figure 8 illustrates the experimental setup for the sulfite oxidation experiments. Gases with known concentrations of NO₂ and/or O₂ in N₂ are lead through a bubbling flask with a prepared batch solution of different salts. Each sample is prepared by weighing each salt and mix into a known amount of degassed milli-q water in an erlenmeyer-bottle. The sample is then sealed and stirred with a magnetic stirrer before it is weighed again to assure correct preparation. The gases, 1% NO₂ in N₂, N₂ and O₂, are supplied by Linde gas. The Bronkhorst MFCs are calibrated for 0 - 0.1 NI/min (O₂), 0 - 0.019 NI/min (NO₂/N₂) and 0-5 NI/min (N₂). The gases are either led directly to the gas analyzer or through the bubble flask. Before each experiment the setup is flushed with N₂ to evacuate O₂. The only O₂ present in the system before experiment initiation is that present in the bubble flask. The bubble flask is equipped with an aeration head, the Raman probe and a pH-electrode. Temperature and chemical composition are measured continuously. The pH electrode is connected to a Metrohm 905 Titrand which is programed to maintain pH at 7 for the samples by addition of 0.1M NaOH. The pH control was, however, unsuccessful during several experiments with resulting pH >9 as too much NaOH was added. The gas analyzer (Testo 350, from Nordtec) measures the concentration of SO₂, O₂, NO and NO₂ by electrochemical sensors on the basis of the selectivity

potentiometry. The amount of absorbed NO_2 is estimated by subtracting the measured exit concentration of NO_2 from the amount injected, which is quantified by a continuous log of supplied mV to the MFC.

The investigated liquid and gas composition is specified in Table 4. SO_3^{2-} and HSO_3^- are added equimolarly to facilitate a neutral pH ~ 7 . SO_4^{2-} is added to investigate if the Raman signal interferes with any of the other species. $\text{S}_2\text{O}_3^{2-}$ is added to investigate the effect it has on S(IV) oxidation. NO_2^- is added to investigate the effect on reaction chemistry and suitability for quantification with Raman spectroscopy. Finally, NO_2 and O_2 are added to oxidize S(IV) and investigate the chemistry of a NO_2 - SO_2 removal system.

Table 4: Evaluated cases in the Raman setup included in this thesis. Amount added and concentrations corresponding to those before equilibrium is reached.

#	SO_3^{2-} (mol/ $\text{kg H}_2\text{O}$)	HSO_3^- (mol/ $\text{kg H}_2\text{O}$)	SO_4^{2-} (mol/ $\text{kg H}_2\text{O}$)	$\text{S}_2\text{O}_3^{2-}$ (mol/ $\text{kg H}_2\text{O}$)	NO_2^- (mol/ $\text{kg H}_2\text{O}$)	CO_3^{2-} (mol/ $\text{kg H}_2\text{O}$)	NO_2 (ppm)	O_2 (%)
1	0.02	0.02	-	-	-	-	-	3
2	0.02	0.02	-	-	-	-	95	3
3	-	-	-	-	-	-	95	3
4	0.02	0.02	-	0.02	-	-	95	3
5	0.02	0.02	0.10	0.04	0.04	0.01	95	3

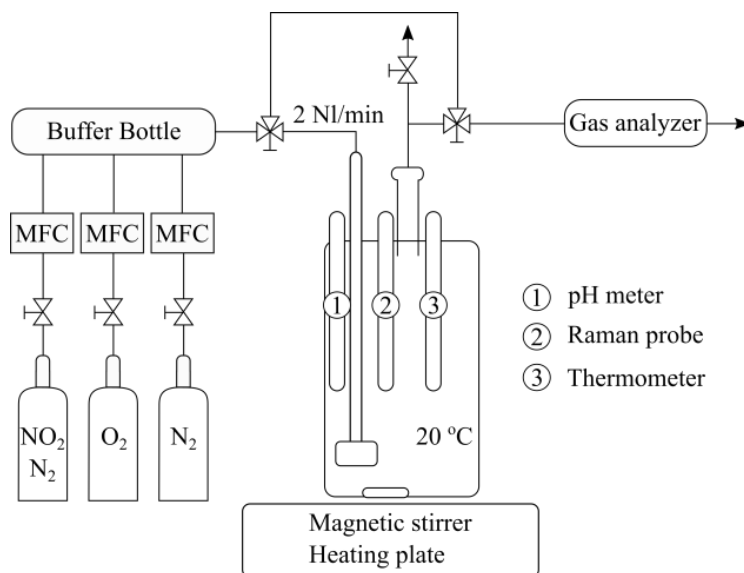


Figure 8: Process outline of the Raman setup. Gases from bottles are mixed at known concentrations and lead to an aerationhead submerged in a bubbleflask. The bubbleflask is equipped with a thermometer, the Raman probe and a pH meter. Gases exiting the bubbleflask are led to a gas analyzer before being released. MFC, Mass flow controller.

2.3 Modeling

2.3.1 Detailed Reaction Mechanism

The modeling is based on previous work in our research group by Ajdari, et al. and the mechanism is described in greater detail elsewhere.⁴

2.3.2 Modeling Assumptions

While the mechanism was developed for the design of pressurized flue gas systems, the reactions are gathered from atmospheric chemistry and as such are within verified conditions. The validation of the reaction mechanism performed herein is a first validation of the compiled model against scrubber experiments. The presence of chloride is completely omitted under the assumption that it will not interfere with the nitrogen and sulfur reactions, except for the inherent influence of the increased ionic strength of the liquid, something which has not yet been studied for this specific case. In any full-scale application, chlorine will most likely be removed in a quench before the scrubber, to avoid the risk of corrosion, which is the case for the 400 Nm³/h unit in the present work.

All the experimental setups have been modeled using the same reaction mechanism. In the models, the flows and their compositions, as well as the scrubber design are set to describe the experimental setups. However, the experiments are not conducted for long enough to reach steady-state operation with respect to the composition of the absorbing liquid. In the 0.2 Nm³/h unit, there is not even a bleed-off from the system, and the amount of absorbing liquid is changing with time depending on the water content of the flue gas. Therefore, the simulations are performed with two approaches, Open Loop and Closed Loop simulations, Figure 9 gives an illustration of the process flow for each approach. The Open Loop simulations are used to test the chemistry in the model. The liquid compositions in the experiments are analyzed and the inlet scrubber liquid compositions in the simulations are set to match the measured concentrations. Since there are no measurements of the S(IV) concentration, alternative strategies are used to set the inlet S(IV) concentration in the simulations. Two methods for controlling the S(IV) concentration in the experimental evaluation simulations are used: 1) The amount of S(IV) in the liquid is set to 0, for experiments in which no Na₂SO₃ is added and assuming all the S(IV) is oxidized in the scrubber liquid tank; 2) the S(IV) concentration is set to the theoretical maximum, for experiments in which Na₂SO₃ is added to the inlet liquid feed, either continuously or in batches.

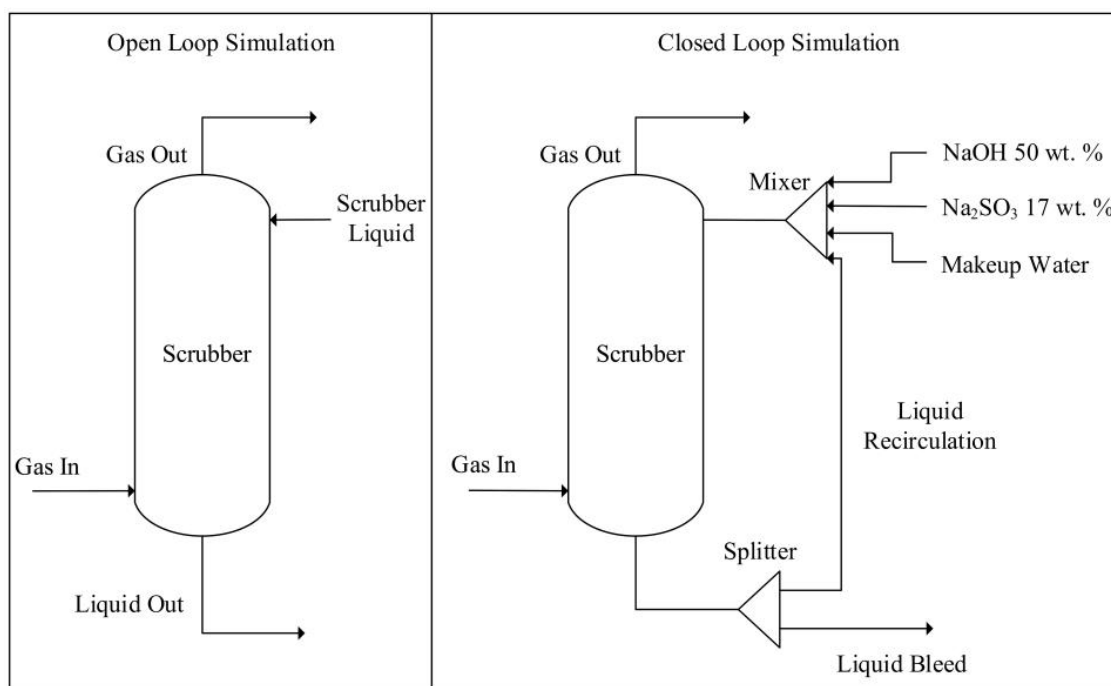


Figure 9: Illustration of the two simulation approaches used: Open Loop (left panel) and Closed Loop (right panel).

The Closed Loop simulations mimic actual operation to evaluate the process performance. It can also be used to assess the Open Loop assumptions with set concentrations. The Closed Loop simulations are performed based on the 400 Nm³/h unit and with emissions regulations for NO_x and SO_x removal targeted. Since the model only oxidizes S(IV) through reduction of NO₂, the amount of S(IV) accumulates if the S/NO₂ ratio is >0.5. The addition of S to the system is therefore controlled so as to originate either from Na₂SO₃ in the liquid or SO₂ in the flue gas, and the resulting S(IV) concentration is always analyzed as a parameter in the results.

In **Paper IV** full scale operation is modeled and cost evaluated for a waste-to-heat plant that is loosely based on the operating data from the plant where the 400 Nm³/h unit was placed. Since cost of operation is an essential piece of the result, an alternative way of treating S(IV) oxidation compared to the previous modeling was chosen to more accurately capture the chemistry observed in experiments. Oxidation of NO via O₂ is added to the reaction mechanism at a rate which corresponds to the highest reported rate found in literature, functioning as a pseudo reaction. Other than this reaction, the chemistry is identical to the previous simulations.

Figure 10 shows the proposed design of the process which is used in the full scale simulations. ClO₂ is injected to the main flue gas path, preferably at a point where the flue gas temperature is 150 ± 10 °C in order to maximize

efficiency and minimize the risk of corrosion. In the conceptual design the oxidation reactor is constructed of Stainless steel 304 L. The reactor should be designed to increase mixing with minimal pressure drop. The flue gas continues to a quench where temperature decrease, and the gas becomes saturated. The quench is maintained at an acidic pH of 1.5 and is of sufficient height to absorb the vast majority of chloride present in the flue gas. A residence time of 5 s is used in this study for design of equipment. The quench is constructed using Stainless steel 6MO/SMO to withstand the harsh environment. The scrubber is designed to achieve 90% absorption of incoming NO_2 . Sodium sulfite (Na_2SO_3) and sodium hydroxide (NaOH) is supplied directly to the liquid feed and not into the scrubber tank in order to minimize reactions with the liquid bulk. In this design, the scrubber is constructed of stainless steel SS2205 to ensure the lifetime of the equipment. The quench and scrubber tank are given dimensions such that it has a volume equal to 3 min of liquid flow. Both tanks are constructed of SS2205. The chemical storage units for NaOH and Na_2SO_3 are designed to hold a volume equal to 1 week of operation. All pumps are centrifugal and sized to fit. The final cost of the acid gas removal system is estimated using Aspen Process Economic Analyzer V11.

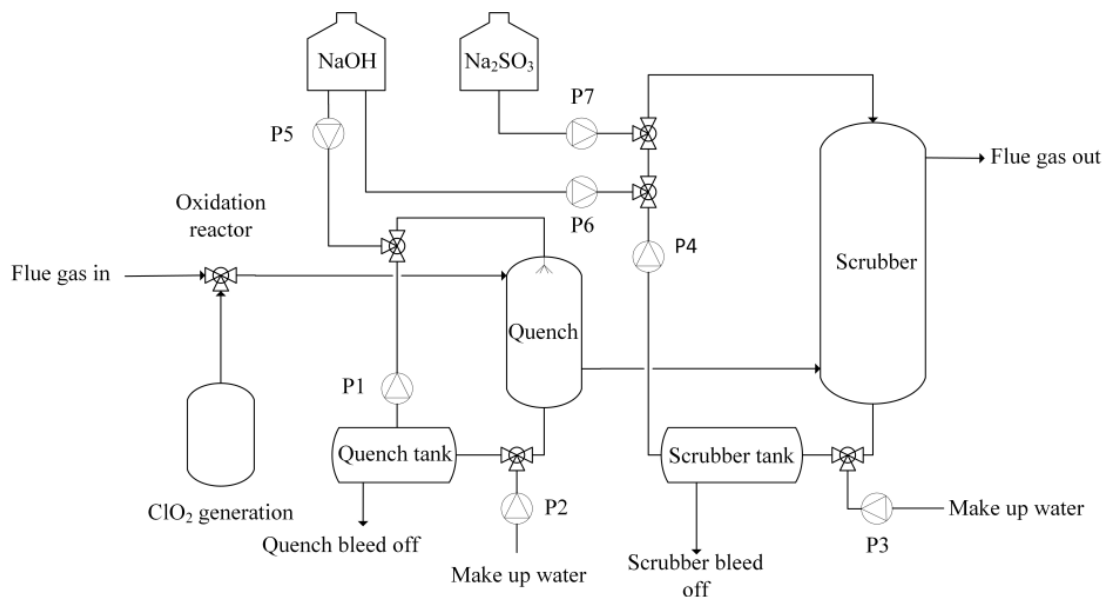


Figure 10: Illustration of the full-scale modeling case of a waste to heat plant. The ClO_2 generation equipment is not included in the cost, only the cost of ClO_2 production.

CHAPTER 3

Conventional Flue Gas Treatment

Commonly used secondary measures to control NO_x emissions are selective catalytic reduction (SCR) and selective non-catalytic reduction (SNCR). Both processes utilize urea or ammonia to reduce NO to N_2 . In SCR, a catalyst lowers the activation energy of the reaction and increase the chemical reduction of NO. SCR operates at a temperature range of $300^\circ\text{--}400^\circ\text{C}$. Without a catalyst a temperature range of $800^\circ\text{--}1100^\circ\text{C}$ is needed to reduce NO. In SNCR, the reducing agent is, therefore, often introduced to the flue gas in proximity to the combustion chamber.

SCR is considered a best available technique (BAT) for NO_x control in large combustion plants. The reduction of NO can reach $>90\%$ depending on the amount of reducing agent used. Strict regulations regarding ammonia slip require stringent control of the process. SCR is considered to have high cost, with the reducing agent, noble metal catalyst, and often the requirement for additional heating all having significant impacts on the running and capital costs. The noble metal catalyst is sensitive to impurities such as SO_2 and dust and is costly to clean and regenerate. This makes implementation of SCR challenging for some applications.

SNCR is considered a BAT for large combustion plants with lower levels of NO_x generation. The avoided cost of a catalyst and direct injection of the reducing agent into the furnace means a reduced capital cost, although this results in a lower reduction potential compared to SCR of only about 50% . The lower reaction rate of non-catalytic reduction requires a larger amount of reduction agent to be injected, as compared to SCR. The unreacted reduction agent may, together with other impurities in the flue gas, form deposits on surfaces downstream, and cause corrosion and plugging and reduced heat transfer in the boiler. Since the reduction potential of NO_x in SNCR is limited, it will not be possible to meet the more stringent emission limits of future legislations.

The removal of sulfur from flue gases may be performed with high efficiency for most applications. The removal often includes calcium, which reacts with sulfur to form stable sulfates. The process can be wet or dry with production of the byproduct gypsum, which is used as a construction material or landfill. The large amount of gypsum produced from wet flue gas desulfurization (FGD) has resulted in market saturations, with consequent drop in price. This may, however, change as an increasing demand for gypsum is

expected.⁷ FGD using a limestone slurry is considered BAT for most large combustion plants. If limestone is readily available close to the site, wet FGD has a relatively low running cost, although it requires large areas for installation and waste disposal.⁸ FGD is not a competing technology to combined NO_x-SO_x removal, it can even be used for this application with some alterations to the current process as will be touched upon in the next chapter. Whether conventional FGD or combined NO_x-SO_x removal will be used for SO_x control will depend on the operating cost and not SO₂ emission limits.

Previous Work and Progress Made

Figure 11 shows an overview of the methods for the five included papers and divide the research field into 4 main categories: NO oxidation, investigated in **Paper I-III**, absorption, investigated in **Paper II-III**, sulfite oxidation, investigated in **Paper V** and the implementation of the proposed technology, investigated in **Paper IV**. This chapter attempts to summarize other literature relevant to my research, divided into the same four main categories.

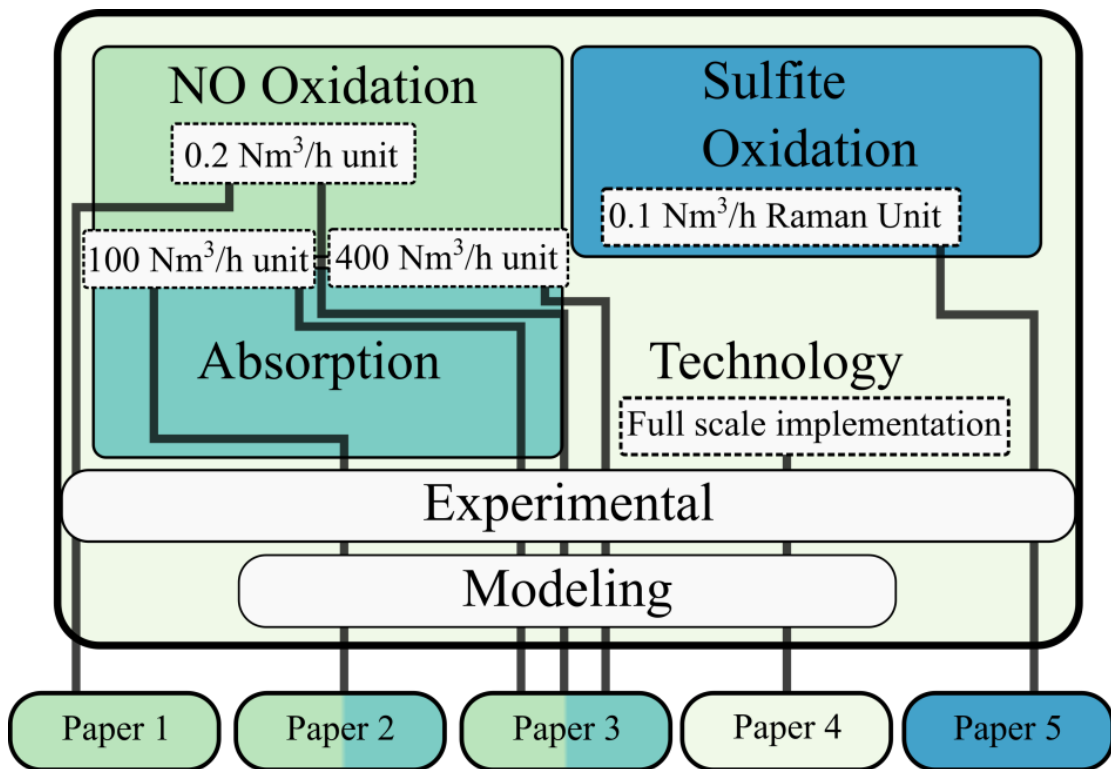


Figure 11: Overview to the thesis. The different methods of the included Papers I-V are indicated with grey lines. Connections are formed between the four main areas investigated (indicated by coloured fields), the four experimental setups, and the proposed full scale design.

4.1 Oxidation of NO to NO₂

The NO_x formed during combustion almost entirely consists of NO. With a very low solubility in water, NO needs to be oxidized to NO₂ or higher oxidation states to facilitate absorption. Research into oxidation of NO, related to NO₂ absorption w/wo SO₂, is here divided into three main categories: gas phase oxidation by oxidizing agents, liquid phase oxidation by oxidizing agents, and oxidation by oxygen at increased pressure.

4.1.1 Oxidation of NO to NO₂ by gas phase oxidizing agents

The oxidation of NO through oxidizing agents in a gas phase reaction enables a high level of control. With addition of the oxidizing agent prior to the scrubber, gas phase measurements can be made to establish the oxidation rate and thereby efficiency of the process. One of the possible oxidizing agents is ozone, O₃. Ozone has a high oxidation potential and can be produced on site with dielectric barrier discharge units. Khalid, O.⁹ tested low-temperature ozone oxidation of NO with the commercial LoTOxTM technology together with oxidation of Hg for absorption purposes. More than > 95% of NO was oxidized at a molar ratio between O₃ and NO <2 and a temperature of 135°C. Ma et al.¹⁰ used O₃ in a lab scale setup with a 2 l/min simulated flue gas flow at ~80°C to oxidize NO to NO₂ for absorption purposes. They identified three oxidation regimes depending on the O₃/NO ratio. Below a ratio of 1.2, NO₂ was the main product. Between 1.2 and 1.7, the reaction goes further (if the residence time was long enough, ~2 seconds) and N₂O₅ forms. At O₃/NO ratios >1.7, the amount of N₂O₅ increased, to eventually represent the majority of the NO_x. Complete oxidation of NO requires an O₃/NO ratio of approximately 2. Jakubiak and Korylewski¹¹ presented results similar to Ma et al.: the residence time and O₃/NO ratio are significant to the reaction product and the same breaking points of 1.2 and 1.7 were identified. They operated their oxidation chamber at 40°C with a flue gas flow of 200 m³/h.

H₂O₂ may also oxidize NO to NO₂ in the gas phase. Kasper et al.¹² investigated the reaction in a quartz reactor at temperatures of 300°-700°C and H₂O₂/NO molar ratios of 0 - 2.7. The optimal oxidation rate was found at 500°C with only a slight efficiency decrease up to 600°C, which can be established as a temperature interval for operation. For complete oxidation of NO a molar ratio of 2.7 between H₂O₂ and NO was required. Chen et al.¹³ proposed a system where Pt-TiO₂ catalysts were used to decompose H₂O₂ at a temperature of ~150°C. With a H₂O₂/NO molar ratio of 12, the NO oxidation was > 98% and 90% of the NO was found as NO₃⁻.

The only published investigations on gas phase oxidation of NO by ClO₂, to my knowledge, is the research included in this thesis. The method and results are discussed elsewhere in this thesis. The key performance numbers for comparison to the other oxidants are: 99% NO oxidation has been achieved in lab and pilot scale units at a molar ratio between NO and ClO₂ of ~0.5. The oxidation is shown efficient in the temperature interval 20°C - 155°C.

Table 5 summarize the NO oxidation rate, oxidizing agent (OA) used and OA to NO ratio. In the included processes, O₃ and ClO₂ are applied at low temperatures and H₂O₂ at high temperatures if there are no catalysts present. All oxidizing agents may efficiently oxidize NO to NO₂. If O₃ is used, further oxidation to N₂O₅ is possible if the OA/NO ratio is increased beyond 1.2. This has not been seen for the other oxidants. The conditions of the flue gas train of the end user and existing infrastructure will determine which oxidizing agent that is most suitable.

Table 5: Summary of methods and efficiency for gas phase oxidation of NO by oxidizing agents.

Method	NO Oxidation Rate	Main active species	OA/NO	Temp	Ref
LoTOx TM /O ₃	>95%	O ₃	2	135 °C	⁹
O ₃	>99%	O ₃	1.2	80 °C	¹⁰
O ₃	>99%	O ₃	2.25	40 °C	¹¹
H ₂ O ₂	95%	•OH	2.7	500 °C	¹²
H ₂ O ₂	98%	•OH, Pt-TiO ₂	12	150 °C	¹³
ClO ₂	99%	ClO, ClO ₂	0.5	150 °C	¹⁴

4.1.2 Oxidation of NO to NO₂ by liquid phase oxidizing agents

If the oxidant used for NO oxidation is produced as a liquid, as is the case for ClO₂ and H₂O₂, liquid phase oxidation has a clear advantage in the ease of how to supply the oxidant to the system. The efficiency and selectivity relative to gas phase oxidation is, however, lower. It should be noted that it is impossible to quantify the liquid phase NO oxidation without also reporting removal efficiency of NO_x as the oxidation and absorption transpires simultaneously, which complicates the direct comparisons with gas phase oxidation.

When using H₂O₂ in a liquid phase system it is often combined with other chemicals or process equipment to increase the generation of hydroxyl radicals at moderate temperatures. Liu et al.¹⁵ proposed an ultraviolet (UV) assisted H₂O₂ system for combined NO, SO₂, and Hg removal operating at 50°C. At 6% O₂, 1500 ppm SO₂, 400 ppm NO, 0.5 M H₂O₂ and 0.003 M Ca(OH)₂ they achieved 80% NO_x removal and 99% SO₂ removal. Liu et al.¹⁶ used a UV-assisted spray reactor with Ca(ClO)₂ to oxidize and absorb NO. The UV radiation increased hydroxyl radical production, which in term increased the process efficiency. A concentration of 0.15 M Ca(ClO)₂ achieved 92% NO removal efficiency. No information is available on additive consumption or

feed rate. Wang et al.¹⁷ used NaClO₂ in a CaO₂ solution to oxidize and absorb NO. With a 0.05 M Na₂ClO₂ concentration all of the NO was oxidized and 92% of the NO_x absorbed. Jin et al.¹⁸ used ClO₂ in an aqueous solution to oxidize and absorb NO in the presence of SO₂. With enough ClO₂ injected, all NO was oxidized and 71% of the NO_x was absorbed. The molar ratio between NO and ClO₂ was not given. The absorption decreases with increasing pH 4-7. Later Deshwal et al.¹⁹ identified that ClO₂(aq) have an increasing absorption rate of NO with increasing pH (8-11) and the disproportionation of ClO₂ was proposed to be the reason behind the decreased absorption rate at a pH between 7-8.

Table 6 summarize the NO removal efficiency and main active species for the included liquid phase NO oxidation studies. In a liquid phase oxidation step, the absorption of NO_x transpires concomitantly with oxidation. Since the molar concentration of oxidizing agents was always greater than the NO oxidized, further oxidation of nitrogen species occur to the extent of what was possible with the oxidation potential of the oxidizing agent. So, while the hydrolysis of NO₂ is a rather slow process, the higher oxidation states formed have a much higher solubility and, thus, reach higher NO_x removal compared to if NO₂ was fed to the scrubber. The oxidizing agents have different oxidizing potential and therefore result in different products in the liquid. When H₂O₂ was used for oxidation, the formed radicals of hydroxyl and oxygen oxidized NO to NO₃⁻ and an acidic pH was beneficial for this reaction. Acidic pH was also reported to be slightly favorable when ClO₂ was used for oxidation. It was suggested that ClO₂ oxidize NO to NO₃⁻, which was the only analyzed nitrogen liquid phase specie. Ca(ClO)₂ was most efficient at a neutral pH and the hydroxyl radicals formed from hypochlorite (HClO) and UV-radiation can oxidize NO₂⁻ to NO₃⁻. When NaClO₂ was used in an alkaline scrubber together with CaO₂, both NO₂⁻ and NO₃⁻ was found as products.

The oxidizing agent used inevitably also oxidize other species, such as SO₃²⁻, if SO₂ is absorbed in the same unit. The consumption of oxidizing agents should therefore in theory be higher in liquid phase oxidation processes compared to gas phase oxidation where selectivity of NO oxidation is easier to control. Unfortunately, the consumption of oxidizing agent was not included in the included studies, so the actual efficiency of the investigated process is difficult to assess.

Table 6: Summary of methods and NO removal efficiency of liquid phase oxidation of NO.

Method	NO removal efficiency	Main active species	Concentration	pH	Ref
UV/H ₂ O ₂ / Ca(OH) ₂	80%	•OH	0.5 M/ 0.003 M	4	15
Ca(ClO) ₂	92%	•OH, HClO	0.15 M	7	16
NaClO ₂ / CaO ₂	92%	ClO ₂ , ClO•	0.05M/ 5 g/l	11	17
ClO ₂	71%	ClO ₂ , ClO•	-	3.5	18
ClO ₂	60%	ClO ₂ , ClO•	-	3.5	19

4.1.3 Oxidation of NO to NO₂ by increased pressure

In the early 2000s, there was increased interest in next-generation combustion technologies for carbon capture and storage (CCS) schemes, such as oxy-fuel combustion and chemical looping combustion (CLC). Soon thereafter it was discovered that the high pressure and low temperature of the CO₂-conditioning train significantly affected the chemistry in the flue gas. The oxidation rate of NO to NO₂ is greatly increased at high pressure due to increased partial pressure of the reacting species.⁶ Since NO₂ is soluble in water, it was found to cause problems during flue gas compression where it dissolved in the formed condensate together with SO₂. White et al.²⁰ proposes a process in which SO_x and NO_x are removed during and after compression in stages; they provided supporting experimental data and termed this process “the sour compression process”. In sour compression, mainly SO₂ is removed in the first stage and NO₂ in the second stage. The process has been further investigated by White et al. and other research groups with alternative designs discussed.^{21–24} Stokie et al.²⁵ evaluated the NO oxidation and subsequent absorption in a pressurized oxy fuel unit where the NO oxidation reached 90% at a pressure of 13.5 bar and a gas residence time of 120 seconds. The O₂ partial pressure was identified as a key parameter for high NO oxidation.

Table 7 summarize the NO oxidation rate achieved at different pressures and residence time from the reviewed studies. Even though the results vary by several orders of magnitude it can with certainty be said that high NO oxidation rates are achievable. The pressure, residence time and O₂ concentration are the main parameters for the rate of oxidation.

Table 7: Summary of method and oxidation rate of NO oxidation caused by elevated pressures.

Method	NO oxidation rate	Pressure	Residence time	Ref
Flue gas compression	96%	15 bar	600 s	21
Flue gas compression	50%	15 bar	-	26
Flue gas compression	0-100%	6-14 bar	-	24
Pressurized combustion/ Direct contact cooler	90 %	13.5 bar	120	25

4.2 Combined Absorption of NO₂ and SO₂

The efficiency of the NO_x and SO_x scrubber is highly dependent upon the established influence of S(IV) on NO₂ absorption.^{27,28} S(IV)_(aq) forms when SO₂ is absorbed into the liquid or if added to the liquid as a salt, and rapidly and efficiently reduce NO₂ to HNO₂. The synergy in the liquid phase between SO_x and NO_x absorption reveals possibilities for a removal technology that is both process- and cost-efficient. The concept of simultaneous removal of NO_x and SO_x for flue gas cleaning applications was first proposed in 1973 and has continued to generate interest. Senjo and Kobayashi applied for a patent for the “Process for removing nitrogen oxides from gas” in 1973, in which it was proposed to oxidize NO to NO₂ with ClO₂ or O₃.²⁹ The intended application was not directly targeted towards simultaneous removal of SO₂, although it was mentioned in the patent as an option.

In subsequent years, many research groups investigated the process or parts of it, with every project concentrating on the oxidation of NO to NO₂. Several groups focused on liquid-phase oxidation of the NO with different oxidizing agents.^{18,30–32} Depending on the agent used, different scrubber pH was required for efficient absorption as was discussed in the previous section. A wide variety of experimental setups have been used with different rates of removal of NO_x being reported (from 3% to 99%). In contrast, the rate of SO₂ removal was always >80%, and often >99% using alkaline scrubber solutions.

Some groups have focused on introducing NO_x absorption into specific, existing FGD processes, such as those involving magnesia and limestone slurries.^{28,33} The attention of the reader was directed to the rapid oxidation of S(IV) that takes place during the absorption process.

Sun et al.³⁴ studied the absorption of NO₂ and SO₂ into a batch sulfite solution. Absorption of both SO₂ and NO₂ diminished with time as SO₃²⁻ concentration was depleted. With the initial concentration of SO₃²⁻ of 0.02 M there was an equal distribution of NO₂⁻ and NO₃⁻ formed from NO₂ absorption. With decreasing SO₃²⁻ concentration ~80% of the absorbed NO₂ formed NO₃⁻.

Kang et al.³⁵ studied NO and SO₂ absorption using O₃ for oxidation of NO in a wet scrubber. They found an optimal NO_x absorption of 65.5% when O₃/NO added was 0.6, pH was 13 and temperature 20°C. They use ion chromatography to analyze the scrubber liquid and find that NO₂⁻/NO₃⁻ was split at 79% and 21% respectively. Zhang et al.³⁶ performed a similar study and achieved 90% NO_x absorption and 99% SO₂ absorption in a batch solution of NaOH. They also use O₃ for NO oxidation, but at a O₃/NO ratio of 1. With decreasing pH from 12 to 3 the NO_x and SO₂ absorption also decrease. Joseph Selinger³⁷ evaluated the removal of low levels of NO₂ (5 ppm) together with SO₂ at 40 ppm in a pilot plant wet scrubber adding Na₂SO₃ for NO₂ absorption and Na₂S₂O₃ to decrease SO₃²⁻ oxidation. With a pH above 8.5 and a S₂O₃²⁻ concentration above 50 mmol/kg the sulfite concentration was maintained at 35 mmol/kg which allowed for 95% NO₂ absorption and 99% SO₂ absorption. Hutson et al.³⁸ used a limestone slurry (WFGD) with addition of NaClO₂ to remove NO and Hg in addition to SO₂. At a temperature of, 55°C, 10% CaCO₃ and 25 mM NaClO₂, with 200 ppm NO, 1500 ppm SO₂ and 206 µg/m³ Hg all of the Hg and SO₂ was captured and 60% of the NO_x. They also identified that the presence of SO₂ and NO was important for the Hg removal and that there was an optimal SO₂ concentration in terms of NO removal. The optimum concentration was assumed to be dependent on the NaClO₂ concentration. Sun et al.³³ investigated the potential for simultaneous removal of SO₂ and NO₂ in a MgO slurry (WFGD). They use O₃ for oxidation of NO before the scrubber. When NO was completely oxidized to NO₂, MgO concentration 25 mM, 200 ppm NO and 500 ppm SO₂, 72% NO_x removal was achieved and 99% SO₂ removal. The scrubber was operated with varying parameters and showed little dependency on pH between 4 and 10. When the O₃/NO ratio was increased, NO_x removal increases due to oxidation of NO₂ to N₂O₅. Sun et al.³⁹ used pyrolusite (MnO₂) as the scrubber addition for SO₂ and NO₂ removal. With 750 ppm NO, 2000 ppm SO₂, a pyrolusite concentration of 500 g/l, 25°C, and scrubber pH of 1, 82% NO_x removal and 90% SO₂ removal was achieved.

Table 8 summarize combined NO_x and SO₂ removal efficiency with the method used for absorption in the reviewed literature. The removal of SO₂ is always >90% due to a high oxidation rate of SO₃²⁻ which is a rate limiting step in conventional WFGD. Depending on scrubber alkalinity and oxidizing agent used the SO₃²⁻ oxidation is governed either by NO₂ absorption or oxidation by the oxidizing agent. In an acidic scrubber, the oxidation of SO₃²⁻ or rather HSO₃⁻, by oxidizing agents is crucial since SO₂ has a low solubility in acidic media and NO₂ interaction with HSO₃⁻ in acidic media is of a low rate. In alkaline solutions, SO₃²⁻ oxidation caused by NO₂ absorption is of a very high rate, eliminating the need of further oxidation measures for SO₂ absorption.

Table 8: Summary of method, NO_x and SO_x absorption efficiency and added species (X) for simultaneous NO₂ and SO₂ absorption systems.

Method	NO _x abs	SO ₂ abs	X	[X]	pH	Ref
Wet scrubber	99%	99%	SO ₃ ²⁻	20 mM	6-7	34
Wet scrubber	70%	99%	ClO ₂	20 mM	4	18
Wet scrubber	65.5%	99%	NaOH		13	35
Wet scrubber	90%	99%	NaOH		12	36
Wet scrubber	95%	99%	SO ₃ ²⁻ , S ₂ O ₃ ²⁻	35 mM, 50 mM	8.5	37
Limestone WFGD	60%	99%	CaCO ₃ , NaClO ₂	10% _w , 25 mM	6.1- 6.7	38
Mg WFGD	72%	99%	MgO	25 mM	6.5	33
MnO ₂ wet scrubber	82%	90%	MnO ₂	500 g/l	1	39
Limestone WFGD	90%	98%	O ₃			40

Much like for SO₂ absorption, the NO₂ absorption scheme is also dependent on pH. Hydrolysis of NO₂ is a rather slow process and for the removal of NO_x to reach >50% the process needs to be enhanced in some way. In acidic media, the oxidizing agent used need to oxidize NO beyond NO₂ to either N₂O₅ or NO₃⁻ which can be removed at a high rate. In an alkaline scrubber, SO₃²⁻ reacts with NO₂ as mentioned and the rate of NO₂ absorption is governed almost exclusively on the SO₃²⁻ concentration.

4.3 Sulfite Oxidation

The focus of the research on sulfite oxidation has with time shifted from atmospheric chemistry due to the high emissions of SO₂, to FGD systems employed to control said emissions and lastly to combined removal systems of NO_x and SO_x. Sensitive systems with complex reaction patterns and with analysis methods that require ex situ measurements, titration, ion chromatography etc. have delivered results that vary with several orders of magnitude.

The oxidation of sulfite has been a debated research question for over a century. Beilke, Lamb and Müller⁴¹ studied the uncatalyzed SO₂-oxidation in a closed environment to investigate rate determining steps in the formation of atmospheric sulfate. Results indicate a first order reaction in regard to sulfite concentration and a zero order in regard to oxygen for a pH between 3-6. Only SO₂ and SO₄²⁻ was measured and S(IV) oxidation was assumed to be rate limiting step. SO₃²⁻ was assumed to be the reacting specie of S(IV) which was

supported by a $[H^+]^{-2}$ trend. They observe no significant dependence on temperature in the interval between 5 and 25 °C. Larson, Horike and Harrison⁴² concurs that the uncatalyzed oxidation of SO_2 by O_2 was first order in SO_3^{2-} but expressed the reaction in terms of an additional H^+ dependence of half order in a pH interval between 4 to 12. Unlike the previous study they did observe a slight temperature dependence in the interval 5 to 25 °C. Connick et al.⁴³ continued the study with focus on the oxidation of bisulfite (pH 4) relevant to flue gas desulfurization (FGD) and atmospheric chemistry, where oxygen concentration and added NaOH was used to determine the reaction path and rate. They suggest that the reaction takes place via HSO_5^- formed from SO_3^{2-} . An expression was formulated for O_2 consumption as second order in HSO_3^- and H^+ and zero order in O_2 . Mo et al.⁴⁴ investigated the sulfite oxidation rate by oxygen and the inhibiting effect on the oxidation by thiosulfate in a thermostatic reactor with continuous air flow. Continuous pH measurements and titration on the resulting liquid was used as a basis for analysis. They noted a decrease in oxidation rate from pH 6 to pH 3 and almost no effect of pH in the interval 7 to 8. The conclusion was that of the previously mentioned studies where the low activity of HSO_3^- will decrease oxidation rate and at a certain concentration of SO_3^{2-} , the reaction was no longer limited by SO_3^{2-} concentration. The effect of $S_2O_3^{2-}$ as an inhibitor for the uncatalyzed oxidation of S(IV) was observed.

The research on S(IV) oxidation in the presence of NO_2 has been performed in parallel to oxidation by O_2 first due to presence of NO_2 in the atmosphere and later coupled to flue gas treatment. NO_2 has a large effect on S(IV) oxidation in the presence of O_2 and the reaction was difficult to study why different approaches has been used and different rates have been proposed. Littlejohn, Wang and Chang⁴⁵ and Rochelle & co-workers^{28,46} has performed a number of studies on sulfite and sulfide oxidation where the influence of NO_2 absorption was investigated. Gas analysis of NO_x was used for determination of reaction rate and the solution was analyzed with ion chromatography.

The research presented in this chapter show that there are a variety of ways to oxidize NO to NO_2 and subsequently absorb it w/wo SO_2 . The methods and performance have constantly been evolving and the technologies are becoming mature. Still, there is limited information available on the scale up of the process and the chemistry involved in the NO_2 - SO_2 absorption process is still debated. This thesis aims to provide answers to some of the questions that are still present.

CHAPTER 5

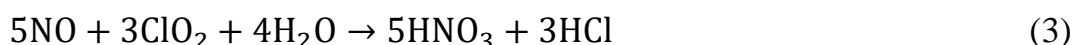
Chemistry

The concept of concomitant absorption of NO_x and SO_x from flue gases includes two important reaction schemes: 1) the oxidation of NO to NO_2 , which increases the solubility of NO_x ; and 2) the liquid-phase interactions of the sulfur and nitrogen chemistry, which facilitate efficient absorption. Figure 12 shows a schematic overview of the proposed reaction scheme. The reactions included are those that are deemed to have significance during the experiments. For a more detailed chemistry, see the work of Ajdari et al.⁴

The gas-phase oxidation is here performed with ClO_2 as the oxidizing agent. The oxidation of NO takes place according to Reactions 1 and 2.⁴⁷⁻⁵⁰ Under dry conditions, Reactions 1 and 2 have a theoretical stoichiometry of 0.5 between NO and ClO_2 .



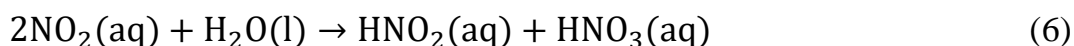
In the presence of water, ClO_2 may be fully reduced to Cl^- , and the theoretical stoichiometry between NO and ClO_2 is then 0.4, according to Reaction 3.



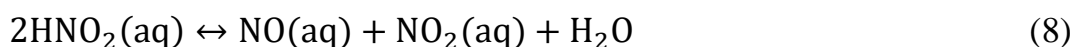
SO_2 absorption in water is equilibrium-controlled and leads to the formation of bisulfite and sulfite according to Reactions 4 and 5, respectively,⁵¹⁻⁵⁴



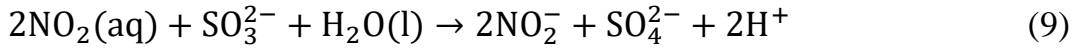
Absorption of NO_2 in water takes place according to either Reaction 6 or 7, depending on the presence of NO and the pH level.⁵⁵⁻⁵⁷



Nitrite, N(III) , is inherently unstable, especially under acidic conditions, and it can decompose into NO and NO_2 :



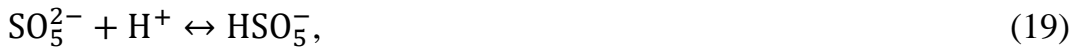
Several studies have shown that S(IV) is efficient at hydrolyzing $\text{NO}_2(\text{aq})$ at a high rate according to Reaction 9.^{34,45,46,58,59}



The SO_3^{2-} may also be oxidized by O_2 following Reaction 10.



In experiments it was found that the oxidation of S(IV) progress at a much higher rate than what is explained by Reactions 9 and 10 alone. Nash⁶⁰ proposed that a radical initiated chain of reactions were initiated by Reaction 9. Littlejohn et al.⁴⁵ proposed the following chain, Reactions 11 to 20.



This set of reactions enables depletion of SO_3^{2-} with only a single SO_3^{2-} radical formed if O_2 is present in the combination of Reactions 15 and 16. To break this chain of reactions a radical scavenger can be added to the liquid which enables an alternative terminating step. One example of such a scavenger is $\text{S}_2\text{O}_3^{2-}$. Shen et al.²⁸ proposed that the formed radical species would react with $\text{S}_2\text{O}_3^{2-}$ and result in production of $\text{S}_4\text{O}_6^{2-}$.



Figure 12 shows a simplified summary of the reaction paths of Reaction 1 to 22 describing a SO_2 - NO_2 absorption process with enhanced oxidation of NO by ClO_2 .

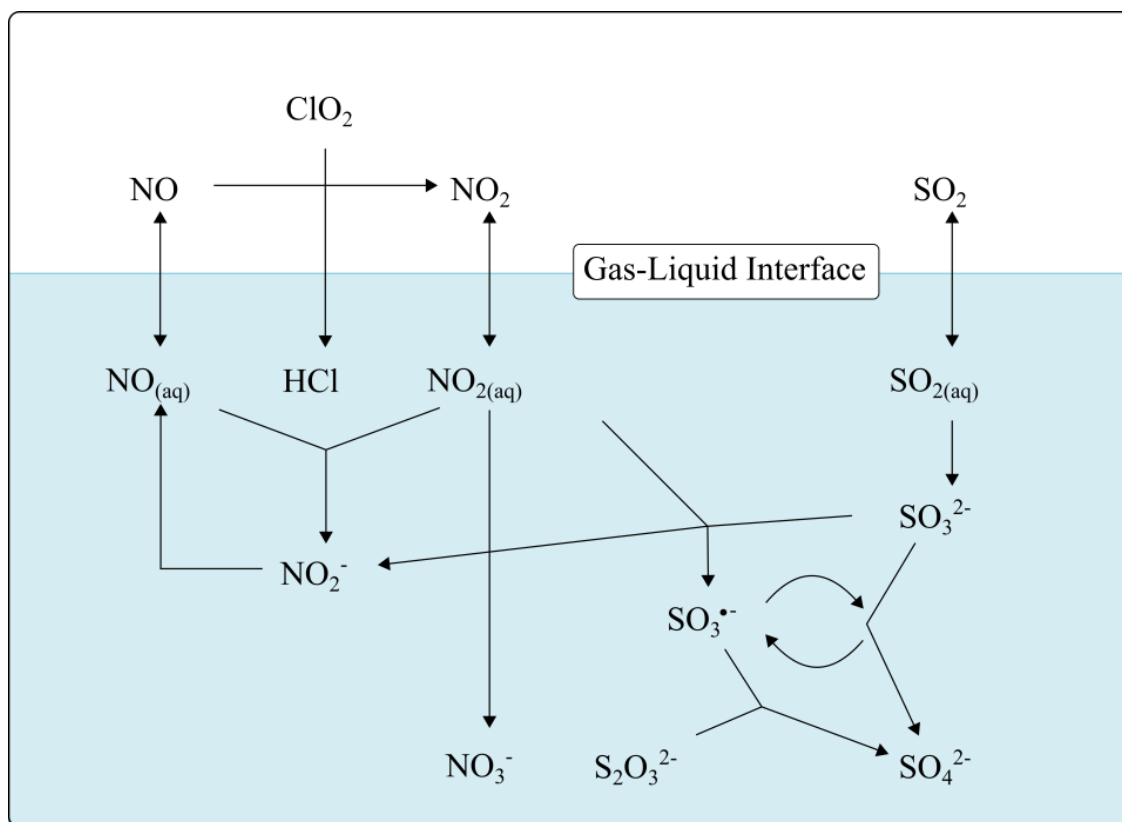


Figure 12: Schematic overview of the chemistry used to describe the simultaneous absorption of NO_x and SO_x after enhanced NO oxidation to NO_2 using ClO_2 . The chemistry is shown for an alkaline pH.

Selected Results and Discussion

This chapter summarizes the most important findings of this thesis. The results are collated from the five appended papers, but also include some unpublished results.

6.1 Validation of the Enhanced Oxidation of NO

Figure 13 shows the measured NO conversion rate against r_{ClO_2} in the three units used in the thesis. The 100 Nm³/h setup delivers the highest conversion at a specific r_{ClO_2} , between 0.4 and 0.5, while the 0.2 Nm³/h and 400 Nm³/h units have a similar and slightly lower rate of NO conversion at a given r_{ClO_2} . All the setups entail the presence of SO₂ in the flue gas, and the 400 Nm³/h setup has a notable concentration of CO. The results show that ClO₂ is selective towards NO oxidation, even when other reducing species are present, since close to all of the NO is oxidized, as compared to the theoretical maximum. The 0.2 Nm³/h setup and the 100 Nm³/h setup are operated at a higher temperature, to avoid condensation in the flue gas train. There is no such control available for the 400 Nm³/h unit, which is why the flue gas holds the temperature equal to the extracted gas minus the heat loss in the piping.

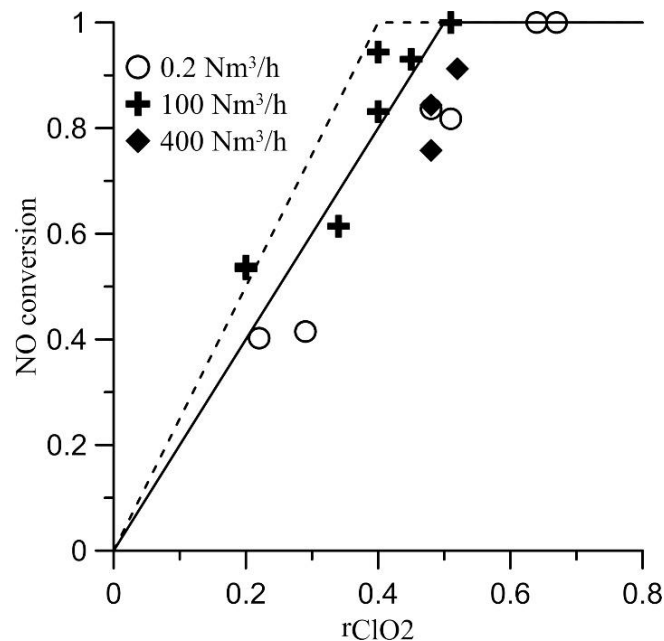


Figure 13: NO conversion rate (Eq 2.2) versus r_{ClO_2} (Eq 2.1). Comparison of the 0.2 Nm³/h, 100 Nm³/h and 400 Nm³/h scales. The solid line shows the theoretical NO conversion rate given a stoichiometry of 0.5 for the ClO₂ and NO ratio (Reactions 1 and 2). The dashed line indicates the maximum theoretical conversion rate (Reaction 3). The results for the 0.2 Nm³/h setup correspond to those shown in Figure 14 c).

Figure 14 shows the influence of H₂O on NO gas-phase oxidation by ClO₂ in the 0.2 Nm³/h setup. The dashed line represents the theoretical conversion rate of NO to NO₂ when all the ClO₂ reacts exclusively with NO and is reduced to Cl⁻, with a stoichiometry of 0.4. The solid line represents the theoretical conversion rate when all the ClO₂ reacts exclusively with NO and is reduced to Cl, with a stoichiometry of 0.5. The experimental results show no major influence of water on NO conversion. It should be noted that even the 0% water case has around ~0.5% water present in the gas, since the ClO₂ is stripped from an aqueous solution. The oxidation of NO is efficient, with rates that are close to or slightly higher than the dry-basis theoretical conversion rate in all cases.

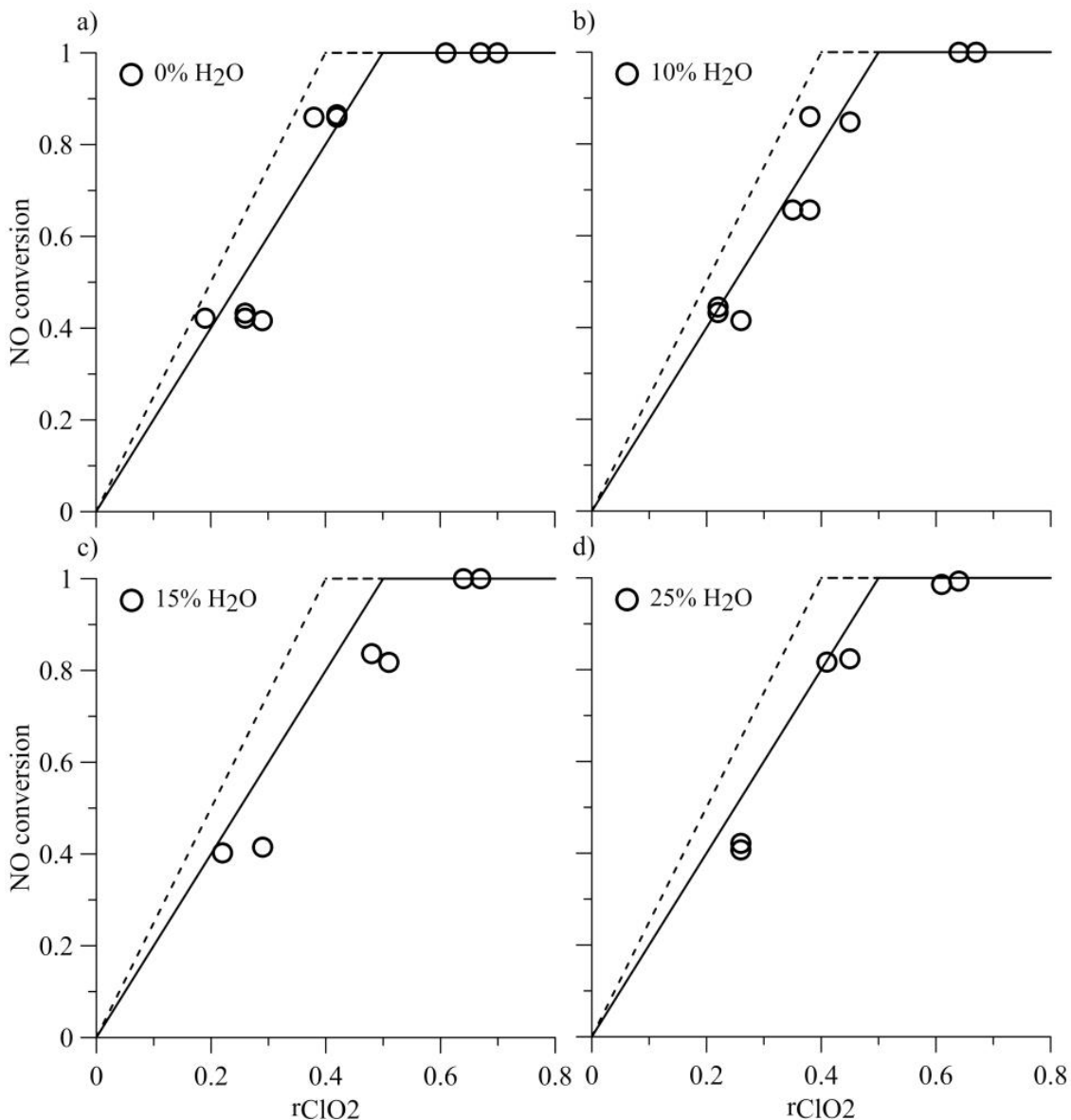


Figure 14: Conversion of NO (Eq 2.2) after ClO₂ injection at the humidity levels: (a) 0% H₂O; (b) 10% H₂O; (c) 15% H₂O; and (d) 25% H₂O at the inlet. Measurements are indicated by circles, and the theoretical dry-basis conversion rate is shown with a solid line in each panel. The theoretical wet-basis conversion is indicated with a dashed line in each panel. Experimental conditions were according to Table 1.

Figure 15 shows the SO₂ conversion rate in the 0.2 Nm³/h setup, as defined by (Eq 2.6). A negative value indicates that more SO₂ is measured after the oxidation than before. Comparing the results in Figure 14 and Figure 15, it is evident that ClO₂ does not oxidize SO₂, while there is NO present for a wide range of water contents. This is vital for the economic feasibility of the concept in that the levels of additives should be minimized. The narrow interval (a matter of few ppm) within which the measurements of SO₂ differ may be attributed to measurement detection limits.

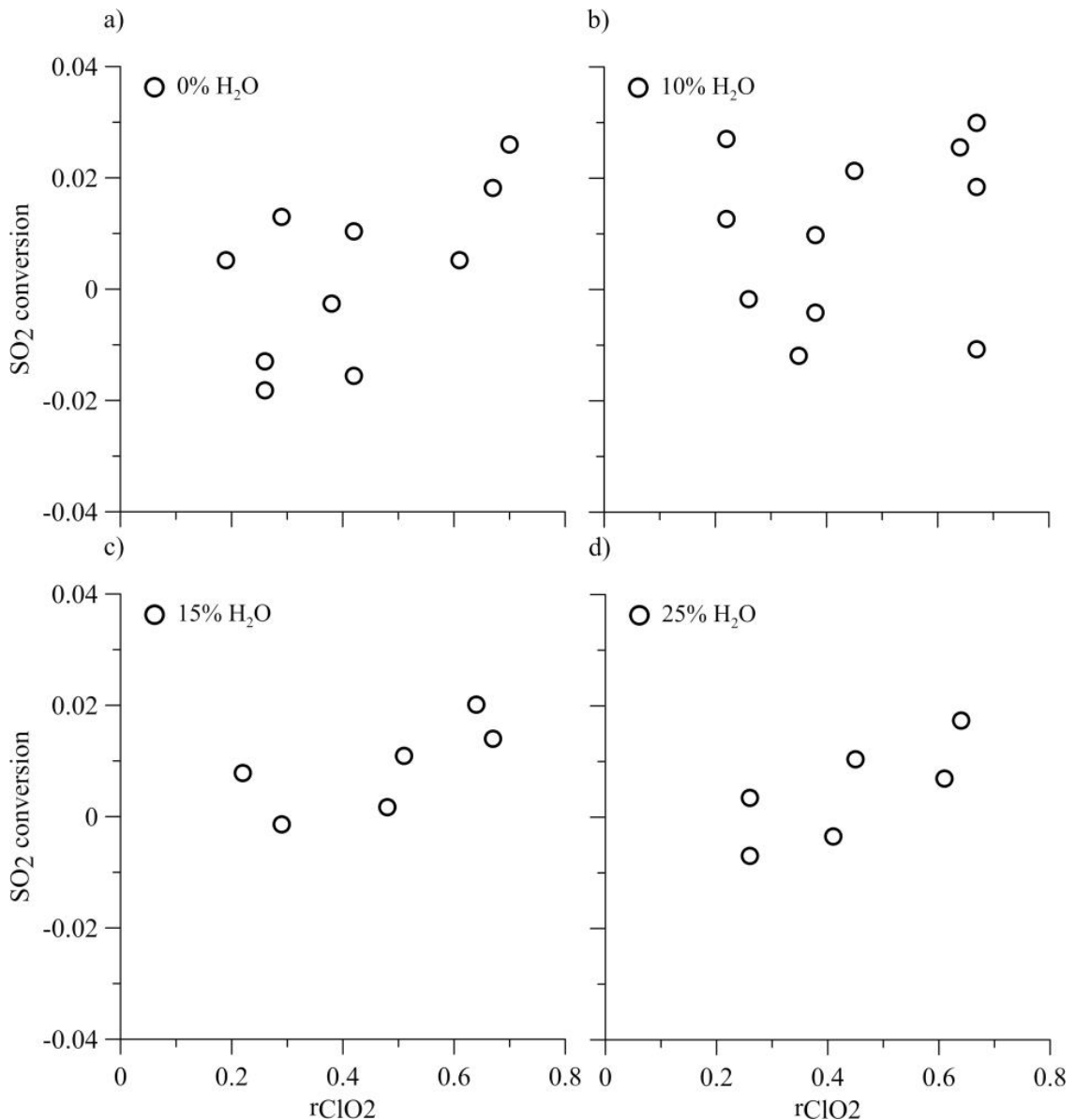


Figure 15: Measured rates of SO₂ conversion (as defined by (Eq 2.6)) between experiments with and without ClO₂ injection at different humidity levels: (a) 0% H₂O; (b) 10% H₂O; (c) 15% H₂O; and (d) 25% H₂O at the inlet. The experimental conditions were according to Table 1.

An inspection of the 100 Nm³/h setup oxidation reactor was performed after approximately 140 hours of operation. Figure 16 shows the photographs from the inspection, together with a color-coded drawing of the oxidation reactor for reference purposes. The ClO₂ injection port was used as the entry point for the camera. In general, there are limited signs of corrosion. The most notable sign is in the upper-right image, showing the insertion pipe for the ClO₂ nozzle. The design renders it prone to stagnation of the flue gas flow. ClO₂ should not be present here since the nozzle is located downstream. No material samples have been analyzed for a more detailed examination, although these photographs indicate that no high-grade materials are needed for the oxidation reactor as long as the temperatures are kept above the acid dew-point.

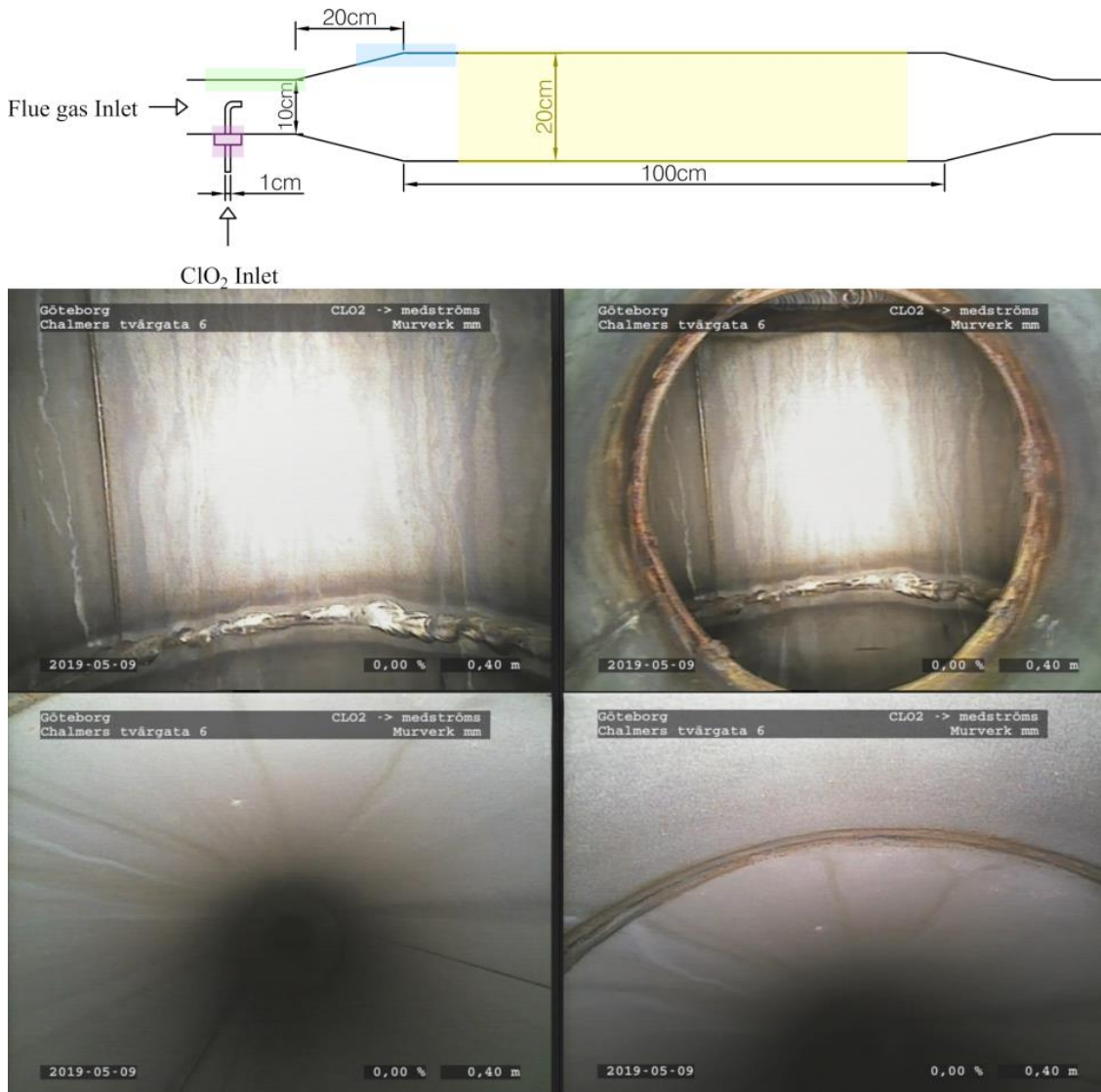


Figure 16: Photographs acquired during the inspection of the oxidation reactor of the 100 Nm³/h setup, together with color-coded legend. Upper-left panel (green): Pipe wall and welding joint at the start of the pipe expansion from 10-cm to 20-cm diameter. A zoomed view of the upper-right image. Upper-right panel (pink): Pipe wall and welding joint at the start of the pipe expansion, as well as the welding joint for the pipe surrounding the ClO₂ injection nozzle (5-cm diameter). Lower-left panel (yellow): Expanded section of the oxidation reactor. Lower-right panel (blue): Welding joint at the end of the pipe expansion.

6.2 Simultaneous Absorption of NO_x and SO_x

The performance and implementation of the process of simultaneous absorption of NO_x and SO_x were evaluated in the three experimental units and through modeling. As expected, the absorption of SO₂ is efficient in all the setups with <10 ppm of SO₂ at the outlet for all trials with alkaline conditions. Under acidic conditions, the saturation of dissolved SO₂ is approached (after sufficient operational time given the used bleed) and SO₂ slip increase. Figure 17 gives the absorption rates of NO₂ without liquid additives besides NaOH for pH control for the 0.2 Nm³/h and 100 Nm³/h setups. The rate of absorption in the smaller unit is higher. The highest NO₂ absorption (no NO is present) achieved without additives in the 0.2 unit is 78%, which is achieved at pH 10 and with a SO₂ concentration in the flue gas of 1,000 ppm (5-times the NO concentration). The improved absorption seen at higher pH levels with higher SO₂ concentrations is significant, whereas the absorption rate remains almost constant for the other cases in the 0.2 Nm³/h unit - only a minor influence exerted by the SO₂ concentration is seen. In the 100 Nm³/h setup, NO₂ absorption is limited (<20%) under acidic conditions. At a pH >7, the NO₂ absorption is improved when the SO₂ concentration in the inlet gas is >400 ppm.

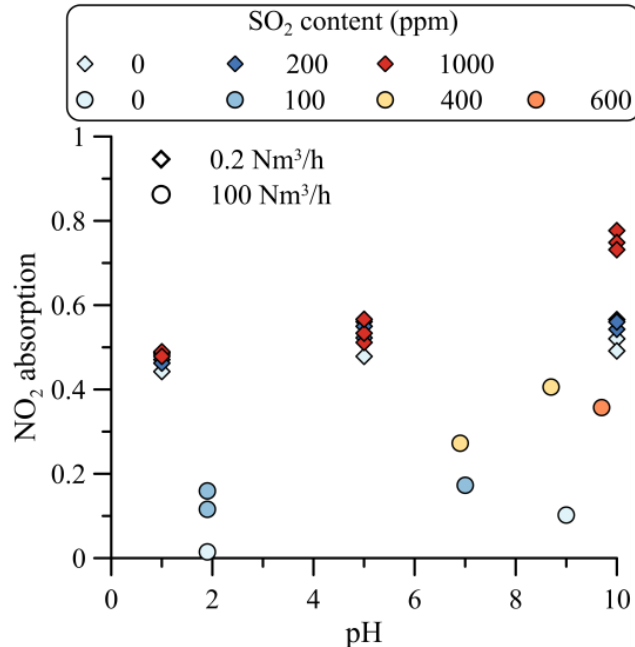


Figure 17: Comparison of NO_x absorption rates, as defined by (Eq 2.3), between the 0.2 Nm³/h and 100 Nm³/h setups operated at different pH levels and SO₂ gas concentrations. The only additive to the liquid is NaOH for pH control. The three inlet concentrations of SO₂ for the 0.2 Nm³/h setup are: 0 ppm, 200 ppm, and 1,000 ppm. The four inlet concentrations of SO₂ for the 100 Nm³/h setup are: 0 ppm, 100 ppm, 400 ppm, and 600 ppm.

NO formation in the scrubber is detected in the 100 Nm³/h setup, most likely due to the instability of N(III) at acidic conditions, whereas this is not seen in the 0.2 Nm³/h unit. At acidic pH, the rate of NO_x absorption, as defined by (Eq 2.3), is 6% and 4%, as compared to the NO₂ absorption, defined by (Eq 2.4), of 16% and 12% due to NO formation in the scrubber. The highest measured rate of NO₂ absorption for the 100 Nm³/h setup is 36%, which is seen at 400 ppm of SO₂ and pH of 8.8. This is the only measurement for which there is no NO formation in the scrubber. The NO₂ absorption is not further improved when increasing the SO₂ concentration at the inlet from 400 to 600 ppm.

Table 9 shows the results obtained from the 0.2 Nm³/h and 100 Nm³/h setups when a 17 wt.% solution of Na₂SO₃ is continuously added to the scrubber liquid at a position close to the inlet nozzles. The indicated S(IV) concentration in the liquid is based on the amount added and assuming that no S(IV) accumulates. High rates of absorption of NO₂ are reached in the two setups. Again, formation of NO in the scrubber is seen in the 100 Nm³/h setup, but not in the 0.2 Nm³/h setup. With the addition of Na₂CO₃ to the scrubber liquid, the formation of NO is decreased; in one experimental case to a point where net absorption of NO is achieved. This indicates that NO is formed from HNO₂ in acidic zones, which are more likely at lower buffering capacity. An alkaline scrubber liquid that has reached steady state should have a fairly limited pH gradient because of all the acid base pairs present, which likely reduce the rate of NO reformation.

Table 9: NO_x absorption profiles for experiments with S(IV) addition to the scrubber liquid inlet conducted in the 0.2 Nm³/h and 100 Nm³/h units.

Setup Nm ³ /h	τ (s)	S(IV) (g/l)	pH	Na ₂ CO ₃ (wt.%)	NO ₂ absorption	NO absorption	NO _x absorption
0.2	6.5	1	9.0	0	91%	0%	91%
0.2	6.5	1	9.0	0	94%	0%	94%
100	9	1	9.5	0	63%	-32%	53%
100	9	1	9.5	0	70%	-94%	59%
100	9	1	8.6	10	71%	-5%	66%
100	15	1	8.8	10	87%	6%	82%
100	9	0.78	7.2	0	85%	-119%	81%
100	9	1.89	7.2	0	74%	-214%	71%

The liquid compositions measured after the experiments were 450 mg/l Cl⁻, 273 mg/l N(III), 250 mg/l N(V) and 10 g/l S(VI). The distribution between N(III) and N(V) is around 1:1. Given the alkaline conditions and that most of the nitrogen is absorbed via Reaction 9, a higher share of N(III) was expected. Oxidation of the nitrogen in the liquid by residual ClO₂ could be an explanation. The amount of residual ClO₂ should however be limited, see Figure 13, and not enough to oxidize the entire amount of nitrogen present. The high concentration of S(VI) is linked to the addition of Na₂SO₃ to the scrubber liquid.

The absorption concept was evaluated under real-world operational conditions in the 400 Nm³/h setup. Figure 18 shows the inlet and outlet concentrations of NO, NO₂ and SO₂ for a period of 2 hours of operation of the 400 Nm³/h unit. There are variations in the inlet concentrations of both NO and SO₂. During the 2 hours of operation, the inlet flow of NO exceeds the amount that it is possible to oxidize with the amount of ClO₂ added over a 20-minute interval, with this occurring after approximately 30 minutes. Otherwise, the NO is completely oxidized in the oxidation reactor. The concentration of NO after the scrubber matches the increase in NO at the inlet, which indicates that no absorption of NO seems to take place. The outlet SO₂ concentration remains constant.

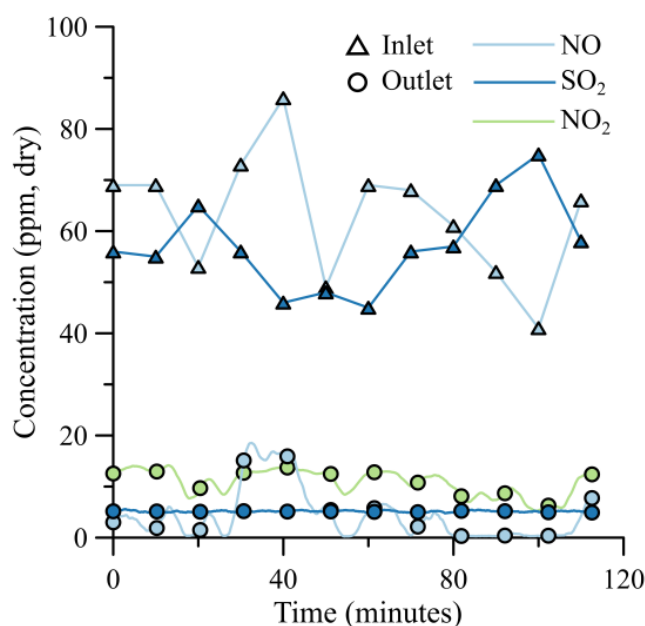


Figure 18: A comparison of the inlet and outlet concentrations of NO, NO₂ and SO₂ during two hours of operation of the 400 Nm³/h unit. Inlet concentrations are measured before ClO₂ injection, and outlet concentrations are measured after the scrubber. The triangles indicate the inlet streams, and the circles indicate the outlet streams. No NO₂ is detected at the inlet (before oxidation). Outlet concentrations are measured every other second while the inlet concentrations are taken as 10-minute interval mean values, i.e., the time resolution is higher for the outlet concentrations.

The scrubber liquid has a continuous feed of 26 l/h of Na_2SO_3 [127 g/l]. The SO_2 absorption rate remains above 90% and the NO_x absorption rate mostly remains above 80%. The results show that the process, while not optimized, can still control the emissions of NO_x and SO_x continuously. However, it should be noted that the amount of Na_2SO_3 added to the scrubber liquid is high. Since the stoichiometry of Reaction 9 gives a theoretical mole ratio of 0.5 for the S(IV) to NO_2 , the added ratio of about 20 is far from optimal.

A similar test was later performed in the same unit at the same facility in Avesta but with addition of a $\text{Na}_2\text{S}_2\text{O}_3/\text{Na}_2\text{SO}_3$ mixture (100g/l and 10g/l respectively) instead of only Na_2SO_3 . In Figure 19 the result of the experiment for a period of 8 hours is visible. The inlet conditions are as can be seen similar to those in the previous experiment but NO_2 absorption is slightly improved. The most significant improvement however is that of the absorption reagent consumption. In this experiment, an average of 0.76 l/h of the $\text{Na}_2\text{S}_2\text{O}_3/\text{Na}_2\text{SO}_3$ mixture was added. The resulting molar ratio for NO_x removed then equals 0.07 for Na_2SO_3 and 0.54 for $\text{Na}_2\text{S}_2\text{O}_3$. As seen for the 0.2 and 100 Nm^3/h units, the presence of SO_2 in the gas phase increase NO_2 absorption through the formed SO_3^{2-} . With the addition of $\text{Na}_2\text{S}_2\text{O}_3$, the SO_3^{2-} formed from SO_2 absorption is more stable and increase NO_2 absorption even more than what is seen in Figure 17.

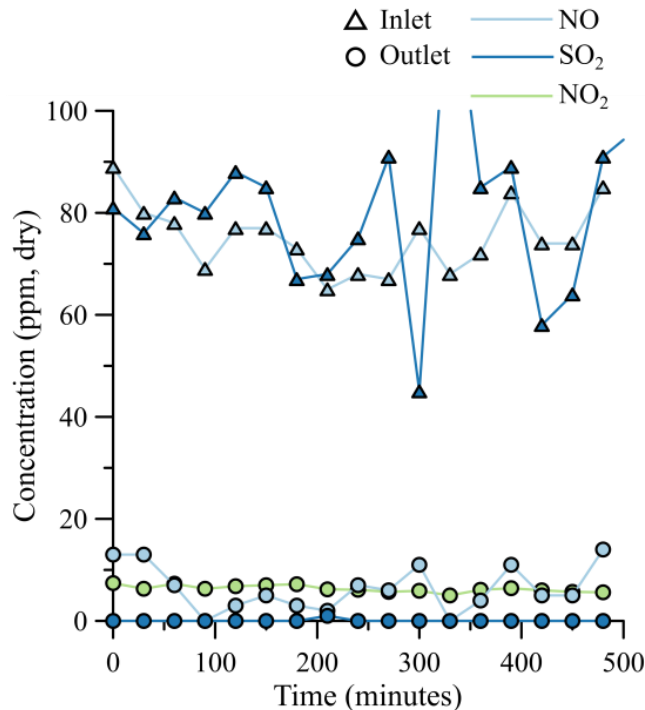


Figure 19: A comparison of the inlet and outlet concentrations of NO , NO_2 and SO_2 during eight hours of operation of the 400 Nm^3/h unit. Inlet concentrations are measured before ClO_2 injection, and outlet concentrations are measured after the scrubber. The triangles indicate the inlet streams, and the circles indicate the outlet streams. No NO_2 is detected at the inlet (before oxidation).

6.3 Validation of the Reaction Mechanism

The reaction mechanism for simultaneous absorption of NO_x and SO_x previously derived by our research group (see Ajdari et al.⁴) was compiled from a series of references from various applications, but was not validated for the present application. The evaluation of the reaction mechanism is, thus, an important outcome of the present experimental campaign.

Figure 20 presents the modeling of the $0.2 \text{ Nm}^3/\text{h}$ setup. For this unit, the mechanism under-predicts the absorption rates, especially under acidic conditions. The model predicts a constant absorption efficiency of approximately 10%, independent of the SO_2 concentration at pH levels <5 . At pH levels >5 , the influence of the bisulfite interactions improves the absorption. Under alkaline conditions, the influence of SO_2 in the gas phase is considerable in both the simulations and experiments, as is evident when comparing the simulation results of $\sim 50\%$ absorption in the case with 1,000 ppm of SO_2 to the $\sim 10\%$ absorption in the case without SO_2 . The main conclusion drawn from this result is that small-scale scrubbers are difficult to represent with the correlations used in the modeling. The discrepancy between modeling and measurements is, however, in accordance with the difference in NO_2 absorption seen between the $0.2 \text{ Nm}^3/\text{h}$ unit and the other two setups, which indicates something that cannot be explained by simply comparing process parameters.

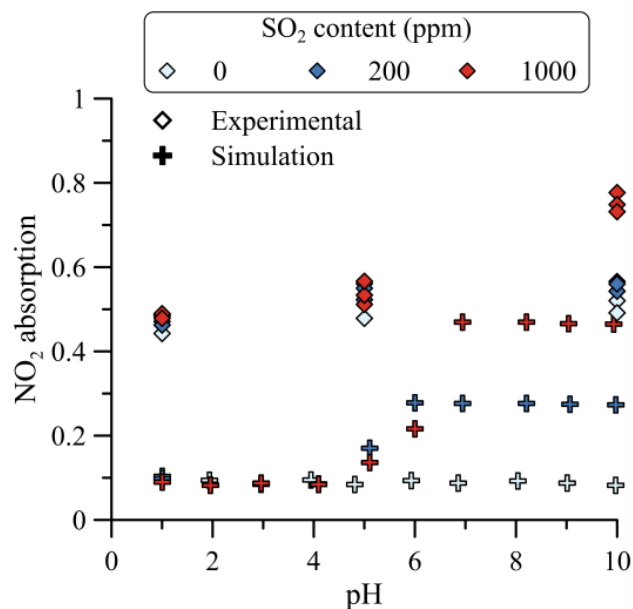


Figure 20: Comparison of the modeling and experimental results presented in Figure 17 for the $0.2 \text{ Nm}^3/\text{h}$ setup. The three inlet concentrations of SO_2 are: 0 ppm, 200 ppm, and 1,000 ppm. NO_2 absorption is defined by (Eq 2.4).

In Figure 21, a comparison of the simulation and experimental results from the 100 Nm³/h unit is shown. The level of agreement between the model predictions and the measurement for this unit is much better than for the laboratory-scale unit. The model, as seen in the results shown in Figure 20, does not capture any influence of SO₂ in the gas phase at pH <5, which explains why all the simulations show an absorber performance that is independent of SO₂ under these conditions. For the experiments conducted under alkaline conditions, the model ably captures the absorption of NO₂. Only one measurement, at pH 8.7, deviates significantly with a simulated absorption of ~30% and an experimental absorption of ~40%. This might be due to as-yet unknown changes in the scrubber liquid, as discussed for Figure 17.

The model does not capture any formation of NO in the scrubber, which is in agreement with the discussion on the importance of local low-pH zones for NO formation as such fluctuations are not present in the model. Reaction 8, which involves N(III) breakdown to NO and NO₂, is favored by high concentrations of N(III) and acidic conditions in the model, which is not seen because the absorption of NO_x, and thereby the concentration of N(III), is limited under acidic conditions. For a liquid with steady-state composition and a more stable pH level throughout the scrubber, little or no NO should be present at the scrubber outlet, which agrees with the model. The results indicate that the model is in good agreement with the experimental data in terms of NO₂ absorption and that simulations without recirculation of the scrubber liquid captures the absorption well.

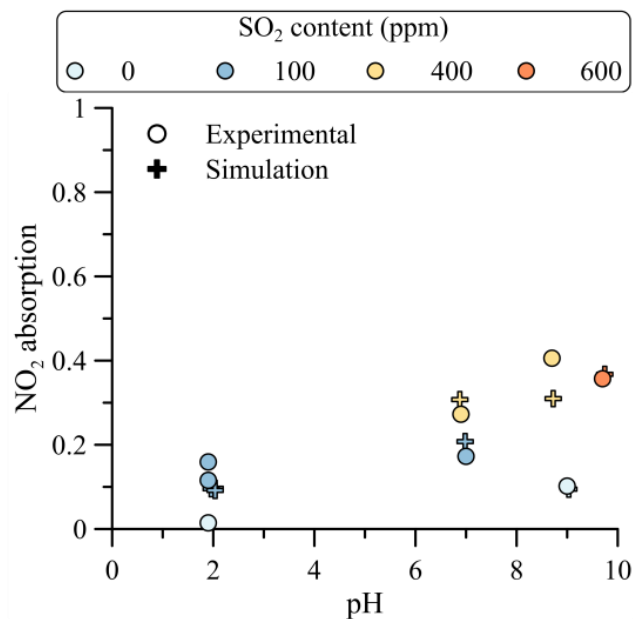


Figure 21: Comparison of the modeling and experimental results presented in Figure 17 for the 100 Nm³/h setup. The four inlet concentrations of SO₂ are: 0 ppm, 100 ppm, 400 ppm, and 600 ppm. NO₂ absorption is defined by (Eq 2.4).

6.4 Modeling of Continuous Operation

Table 10 presents the composition of the liquid bleed for the simulation of the waste-to-heat plant with 150 ppm wet NO₂ and 150 ppm wet SO₂. The absorption rates of NO₂ and SO₂ are required to be 90% and >99%, respectively. The level of liquid bleed is governed by the S(VI) concentration in the scrubber liquid, to avoid the formation of solids. The final NO₂ absorption is controlled by the addition of Na₂SO₃ and pH is adjusted by addition of NaOH. The remaining results are following of the three governing parameters mentioned above.

Table 10: Inlet conditions and resulting concentrations of the components of the scrubber liquid bleed from the simulated WTHP during Closed Loop simulations. The S(IV)/NO₂ ratio is based on moles SO₂ absorbed and moles Na₂SO₃ added to the scrubber liquid.

Parameter	Value
Set values	
SO ₂ removal efficiency (%)	>99
NO ₂ removal efficiency (%)	>90
Raw Flue Gas Flow (Nm ³ /h)	57,500
N ₂ (%)	65
CO ₂ (%)	8
H ₂ O (%)	16
O ₂ (%)	11
SO ₂ (ppm wet)	150
NO ₂ (ppm wet)	150
Scrubber liquid pH	7.2
Resulting flows	
Liquid Flow (m ³ /h)	575
L/G (kg liquid/kg gas)	10
NaOH (l/hr)	58
Na ₂ SO ₃ (l/hr)	60
S(IV)/NO ₂ (mole/mole)	1.3
ClO ₂ (kg/hr)	8.5
SO ₂ removed (kg/hr)	20
NO ₂ removed (kg/hr)	13
Make up water (m ³ /h)	1.34
Liquid bleed (m ³ /h)	1.38
N(III) (g/l)	8.8
N(V) (mg/l)	36
S(IV) (mg/l)	60
S(VI) (g/l)	25
HADS (g/l)	2.7
Carbonates (g/l)	1.8

With the added pseudo reaction of S(IV) oxidation from O_2 , S(IV) is no longer only accumulating if the S(IV)/ NO_2 ratio is above 0.5 as it does in the original mechanism. The pH is set to 7.2 due to experimental experience from the 400 Nm^3/h unit and due to observed maximum absorption of NO_2 in simulations. With a decreased pH, the amount of absorbed carbonates would decrease and likewise the need for added NaOH.

The optimal design found during simulation was used as a basis for the cost-estimation using Aspen Process Economic Analyzer V11. The cost optimal scrubber height was decided to 32 meters as a trade of between process chemicals and equipment cost. Figure 22 shows selected results of the cost estimation for the acid gas removal. The left figure shows the removal cost of the acid gases NO_2 and SO_2 in €/ton removed divided between cost categories. The total cost is estimated to 2,100 €/ton SO_2+NO_2 . The NaOH consumption for pH control is a major cost. It would be possible to lower the NaOH consumption by operating at a lower pH and decrease the absorption of CO_2 . The margins are, however, small since most of the NaOH is added to neutralize the absorbed NO_2 and SO_2 as well as the HCl formed from the added ClO_2 . Electricity-, water- and ClO_2 consumptions are stable, and the cost should mainly vary with consumer price. ClO_2 consumption is at the theoretical minimum for complete NO to NO_2 oxidation. Water consumption is based on S(VI) concentration in the scrubber bleed and 70% of the S(VI) is from absorbed SO_2 . Na_2SO_3 consumption and capital costs are, thus, the only cost categories possible to affect in cost optimization.

To the right in Figure 22, the total direct cost, which is the basis for the capital cost, is given. The scrubber cost is almost 75% of the total direct cost. The scrubber is high and constructed of high-grade materials (SS2205). A high scrubber requires less Na_2SO_3 to reach 90% NO_2 absorption; there is, thus, a tradeoff between chemical consumption and scrubber height important to the removal cost. The S(IV)/ NO_2 molar ratio equals 1.3 in this simulation of which 0.3 is added through Na_2SO_3 . The experiments of Figure 19 have a 4.8 meters column and around 0.07 moles S(IV) per mole NO_2 added through Na_2SO_3 together with 0.54 moles of $Na_2S_2O_3$ per mole of NO_2 absorbed. The ratio of added sulfur was, thus, more than halved in the modelling, but the scrubber is around 6 times as high. To improve the simulations, kinetics for the NO_2 - $S_2O_3^{2-}$ and the S(IV)- $S_2O_3^{2-}$ interaction needs to be developed.

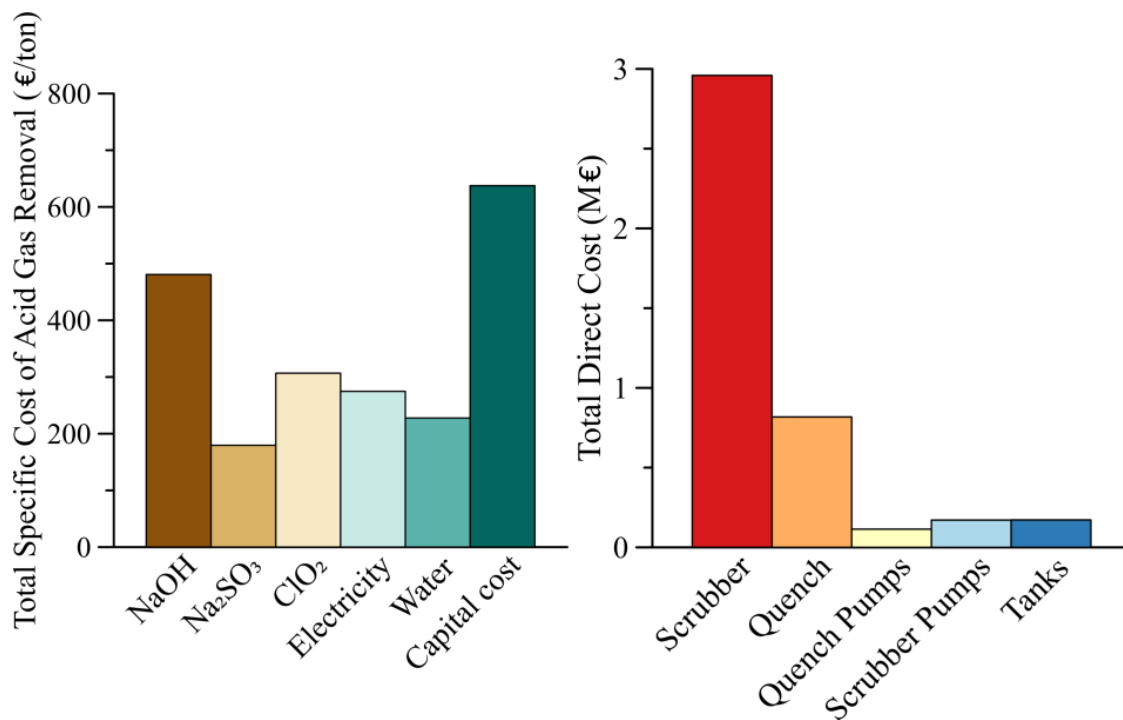


Figure 22: Cost estimations for the 20 MW_{th} waste-to-heat plant. To the left, the absolute total specific cost of combined SO₂/NO₂ removal in €/ton removed. To the right the total direct cost of equipment for combined SO₂/NO₂ removal in M€.

6.5 On-line monitoring of sulfite oxidation

The role of S(IV) in NO₂ absorption and the complex reaction kinetics it involves are a central theme throughout this work. In **Paper V**, Raman spectroscopy was used in the 0.1 Nm³/h setup as a tool for online monitoring of the reactions taking place in a NO₂-S(IV) liquid system.

Figure 23 shows time dependent concentration profiles for SO₄²⁻, SO₃²⁻ and HSO₃⁻ for three cases: S(IV) oxidation via O₂ (solid line), S(IV) oxidation via O₂ and NO₂ (triangles) and S₂O₃²⁻ inhibited S(IV) oxidation via O₂ and NO₂ (crosses). SO₄²⁻ is the main product of S(IV) oxidation, either through Reaction 9 or Reaction 10. The formation of SO₄²⁻ in the left figure corresponds well with the consumption of SO₃²⁻ and HSO₃⁻. The rate of SO₄²⁻ formation is roughly 10 times higher during NO₂ absorption compared to when only O₂ is present in the gas phase. The molar ratio between formed SO₄²⁻ and absorbed NO₂ is ~30, which shows that Reactions 9 and 10 alone are not enough to describe the active liquid phase chemistry. The results are not proving the proposed radical chain propagation, Reactions 11-22, although they are in agreement. Addition of S₂O₃²⁻ to the liquid significantly reduces the rate of SO₄²⁻ formation, which further strengthens the validity of the proposed radical chain propagation for S(IV) oxidation and the inhibiting effect of S₂O₃²⁻. When S(IV) is solely

oxidized by O_2 , SO_3^{2-} seem to be the reacting specie, while HSO_3^- concentration remains constant. This agrees with the assumption made by Beilke, Lamb and Müller⁴¹, that the oxidation of SO_3^{2-} to SO_4^{2-} occurs by a first order reaction in SO_3^{2-} and that no oxidation of HSO_3^- occurs directly. When NO and O_2 is present, both SO_3^{2-} and HSO_3^- are consumed showing that the absorption of NO_2 occurs by a reaction with both SO_3^{2-} and HSO_3^- . The Raman signal for SO_3^{2-} and, to some extent, HSO_3^- are connected to considerable amounts of uncertainty due to the broad nature of the Raman peaks analysed. However, the sulphur molar balance is completed at all times, which shows the success of the measurement technique for on-line measurements of S(IV) in a reacting NO_2 - SO_2 absorption system.

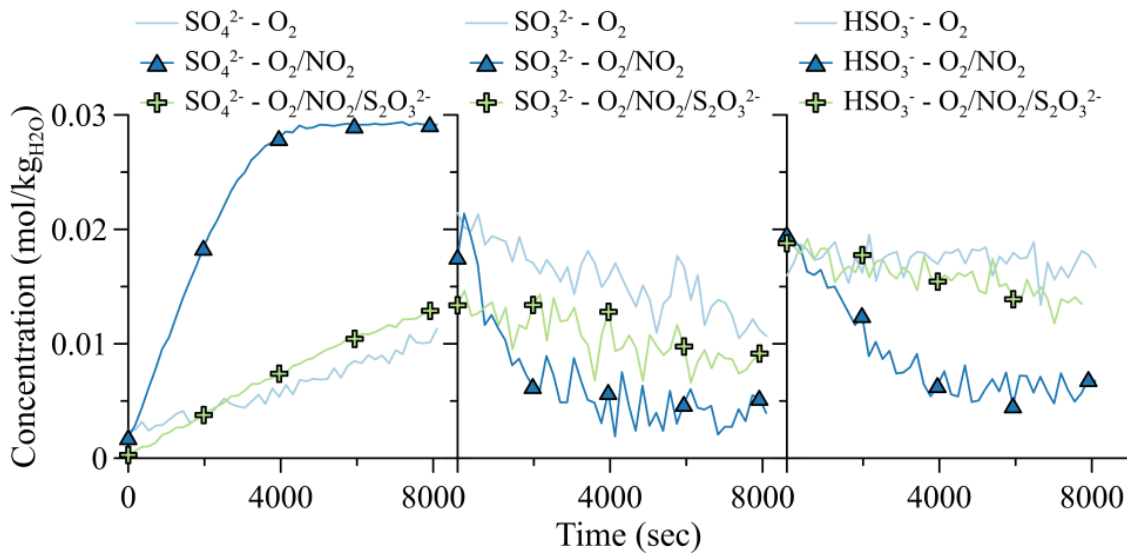


Figure 23: Concentration profiles of SO_4^{2-} , SO_3^{2-} and HSO_3^- during experiments where O_2 (solid line) or a mixture of O_2 and NO_2 (triangles) is used to oxidize S(IV). $Na_2S_2O_3$ is added to inhibit the said oxidation (crosses).

Figure 24 shows the NO_2 and NO_x (NO_2+NO) concentration of the outlet gas from the experiments shown in Figure 23 (except that the O_2 only experiment is exchanged with a pure water experiment to show the effect of the absorption unit on NO_2 absorption). After the NO_2 gas is injected to the bubble flask there is a short time period where the system stabilizes after which the outlet concentration of both NO_2 and NO_x steadily increase. The bubbleflask has a baseline absorption of NO_x at $\sim 6\%$ and NO_2 at $\sim 17\%$. All NO_x is NO_2 at the inlet to the bubble flask. This implies that NO is formed from the absorbed NO_2 , something that was also observed in the $100 \text{ Nm}^3/\text{h}$ unit. It is most likely that it progresses in the liquid film according to Reaction 7, which is active due to local acidic pH. With a starting concentration of S(IV) at 0.04 M , about 75% of the NO_x is absorbed. The absorption is decreasing rapidly with time as S(IV) is oxidized to SO_4^{2-} . At the end of the experiment ($8,000$ seconds) the NO_x absorption is equal to the NO_x absorption in water. The amount of released NO is almost constant until S(IV) is close to depleted ($5,000$ seconds) after which it rapidly increases. When $\text{S}_2\text{O}_3^{2-}$ is added to the liquid the rate of S(IV) oxidation decreases and NO_x absorption decrease at a much slower rate compared to when only Na_2SO_3 is added.

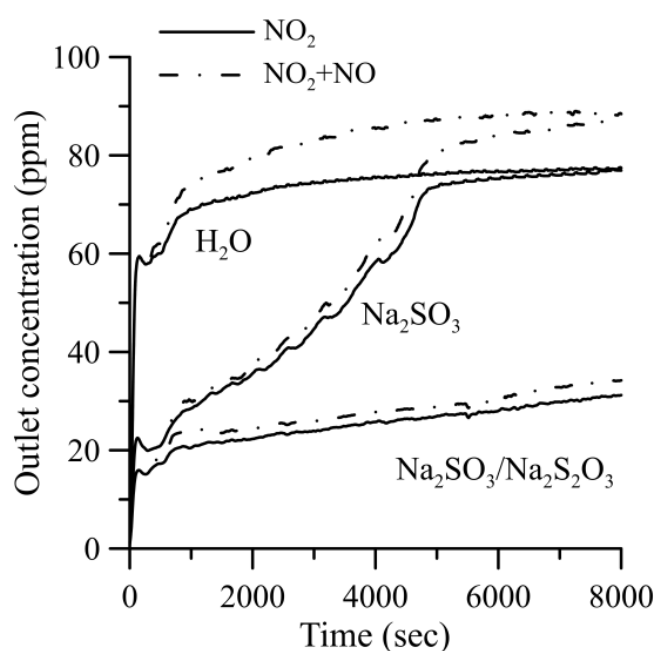


Figure 24: The NO_x absorption over time in the Raman test setup for three liquid compositions: 0.04 M of Na_2SO_3 , 0.04 M S(IV) with 0.04 M $\text{Na}_2\text{S}_2\text{O}_3$ and clean water for reference.

Figure 25 show the correlation between S(IV) concentration and NO_x absorption in the Raman setup. The included results are from the two experiments with Na_2SO_3 included in Figure 24 as well as an experiment where CO_3^{2-} and NO_2^- is added in addition to Na_2SO_3 and $\text{Na}_2\text{S}_2\text{O}_3$. The results show that NO_x absorption is mainly dependent on S(IV) concentration and not effected by the other additives. While the concentration of S(IV) is above ~ 0.015 M there is a proportional correlation between NO_x absorption and S(IV) concentration. Below 0.015 M of S(IV) the NO_x absorption decreases to below 40% and decrease further without a clear correlation to S(IV) concentration. The results with NO_x absorption below 40% have such a large deviation in NO_x absorption due to the increased release of NO visible in Figure 24.

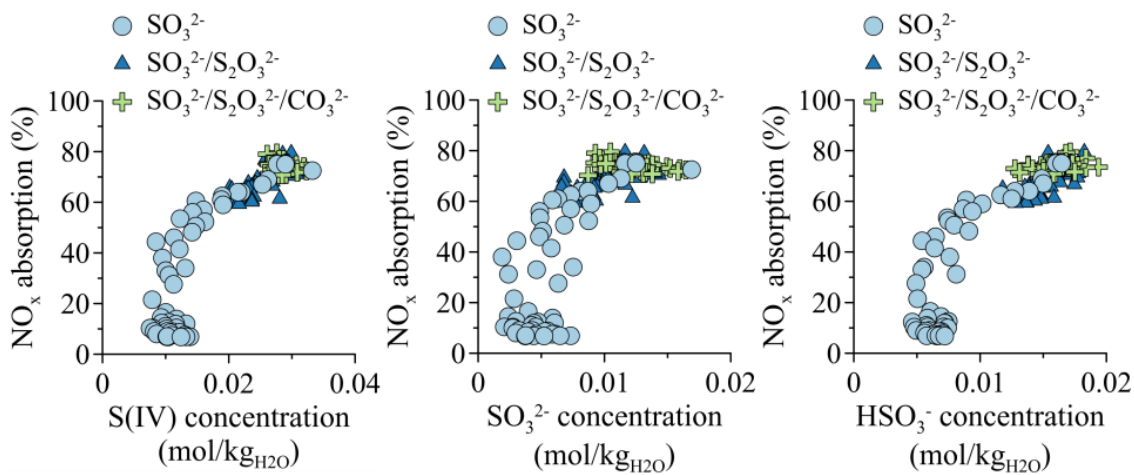


Figure 25: Concentration of S(IV), SO_3^{2-} and HSO_3^- plotted against the achieved NO_x absorption. Baseline absorption without S(IV) is 6%.

CHAPTER 7

Conclusions

This work investigates the simultaneous absorption of NO_x and SO_x from flue gases (**Papers II-V**) in a process that employs enhanced oxidation of NO to NO_2 by ClO_2 (**Papers I-III**). The work has erected four experimental units to study the scale-up of the process and the related chemistry ranging from laboratory bench scale to industrial slip stream trials. The main conclusions drawn from the results of these studies are presented below.

For a flue gas at low temperatures ($<200^\circ\text{C}$), it is concluded that *NO is efficiently oxidized to NO_2 by ClO_2 gas to complete conversion through fast gas-phase reactions at a ClO_2/NO molar ratio of ~ 0.5 . This should be compared to the stoichiometric ratio of 0.4 that is required under ideal and wet conditions. The selectivity of ClO_2 towards NO oxidation is high in the investigated environments. There are no indications of SO_2 or CO oxidation in any of the experimental setups. Furthermore, it can be concluded that the concentration of water in the flue gas exerts no effect on the degree to which NO is oxidized.*

The absorption of SO_2 is near-complete in all the units under alkaline conditions. The absorbed NO_2 oxidize SO_3^{2-} and HSO_3^- to SO_4^{2-} in a fast reaction which enhance the SO_2 absorption by shifting the SO_2 - SO_3^{2-} equilibrium. The absorption of NO_2 under alkaline conditions is, across all scales, highly dependent on amount of SO_2 in the gas phase and addition of Na_2SO_3 to the liquid. The relation between sulfur and NO_2 absorption is confirmed by the computer modeling of the two larger setups.

SO_3^{2-} oxidation competing with NO_2 absorption is crucial to the process performance. The work shows that Raman spectroscopy is a viable method for on-line concentration measurement of SO_3^{2-} , HSO_3^- , SO_4^{2-} and $\text{S}_2\text{O}_3^{2-}$. It is confirmed through experiments that NO_2 absorption triggers SO_3^{2-} and HSO_3^- oxidation through a radical chain and that $\text{S}_2\text{O}_3^{2-}$ is efficient at canceling this radical chain.

The removal efficiencies of the co-absorption system may reach the level of what is currently considered best available techniques, with $>90\%$ and $>99\%$ removal for NO_x and SO_2 , respectively. Cost efficiency is increasing with increasing SO_2 concentrations in the flue gas. Optimally no addition of SO_3^{2-} is needed through salts. The cost of removal for NO_2 and SO_2 is estimated to 2100 €/ton (NO_2+SO_2) for a 20 MW_{th} waste-to-heat plant.

CHAPTER 8

Suggestions for Future Work

Based on the discussion and conclusions of this work, the key areas where there is still a crucial knowledge gap related to the co-removal of NO_x and SO_x are as follows:

Treatment of the scrubber effluent. There is to date no efficient way of treating a liquid containing both S and N salts and the destruction of the effluent is therefore potentially a great unknown cost and a limit to the environmental benefits of the proposed technology. Further studies are therefore required to establish methods of efficient scrubber effluent treatment.

Catalyzed sulfite oxidation. The presence of S(IV) in the absorbing liquid is crucial for efficient NO_2 removal. The oxidation inhibition of S(IV) by $\text{S}_2\text{O}_3^{2-}$ is demonstrated and understood but the influence of other catalysts on the oxidation is still a work in progress. More work is therefore needed on the effect of different catalysts that can be present in industrial flue gases to be able to properly design pre-processing steps.

The on-line measurement of liquid composition by Raman spectroscopy is only started in this thesis. There is still more work to properly establish a model for more precise quantification. The analysis method could potentially be used for the more complex liquids that are present in a flue gas cleaning system, something that needs to be studied. Further usage of the analysis method includes process control/optimization of a NO_x - SO_x removal system and detailed studying of additional components of interest in the system, for instance Hg removal.

Bibliography

- (1) WHO. *Ambient Air Pollution: A Global Assessment of Exposure and Burden of Disease*"; 2016.
- (2) EEA. *Air Quality in Europe - 2019 Report*; EEA, 2019.
- (3) IEA. *World energy balance and statistics*. <https://www.iea.org/data-and-statistics>.
- (4) Ajdari, S.; Normann, F.; Andersson, K.; Johnsson, F. Reduced Mechanism for Nitrogen and Sulfur Chemistry in Pressurized Flue Gas Systems. *Ind. Eng. Chem. Res.* **2016**, *55* (19), 5514–5525.
- (5) Andersson, K.; Johansson, R.; Johnsson, F.; Leckner, B. Radiation Intensity of Propane-Fired Oxy-Fuel Flames: Implications for Soot Formation. *Energy & Fuels* **2008**, *22* (3), 1535–1541.
- (6) Ajdari, S.; Normann, F.; Andersson, K.; Johnsson, F. Modeling the Nitrogen and Sulfur Chemistry in Pressurized Flue Gas Systems. *Ind. Eng. Chem. Res.* **2015**, *54* (4), 1216–1227.
- (7) Layr, K.; Hartleib, P. Market Analysis for Urban Mining of Phosphogypsum. *B. Huettenmaenn Monatsh* **2019**, *164* (6), 245–249.
- (8) Oskarsson, K.; Berglund, A.; Deling, R.; Snellman, U.; Stenbäck, O.; Fritz, J. J. A Planner's Guide for Selecting Clean-Coal Technologies for Power Plants. *World Bank Technical paper NO. 367*. The World Bank 1997.
- (9) Omar, K. *Evaluation of BOC's LoTOx-TM Process for the Oxidation of Elemental Mercury in Flue Gas from a Coal-Fired Boiler*; 2008.
- (10) Lin, F.; Wang, Z.; Ma, Q.; He, Y.; Whiddon, R.; Zhu, Y.; Liu, J. N₂O₅ Formation Mechanism during the Ozone-Based Low-Temperature Oxidation DeNO_x Process. *Energy and Fuels* **2016**, *30* (6), 5101–5107.
- (11) Jakubiak, M. P.; Kordylewski, W. K. Pilot-Scale Studies on Nox Removal from Flue Gas via No Ozonation and Absorption into Naoh Solution. *Chem. Process Eng. - Inz. Chem. i Proces.* **2012**, *33* (3), 345–358.
- (12) Kasper, J. M.; Clausen, C. A.; Cooper, C. D. Control of Nitrogen Oxide Emissions by Hydrogen Peroxide-Enhanced Gas-Phase Oxidation of Nitric Oxide. *J. Air Waste Manage. Assoc.* **1996**, *46* (2), 127–133.
- (13) Chen, L.; Xu, Z.; He, C.; Wang, Y.; Liang, Z.; Zhao, Q.; Lu, Q. Gas-Phase Total Oxidation of Nitric Oxide Using Hydrogen Peroxide Vapor over Pt/TiO₂. *Appl. Surf. Sci.* **2018**, *457*, 821–830.
- (14) Johansson, J.; Hulten, A. H.; Ajdari, S.; Nilsson, P.; Samuelsson, M.; Normann, F.; Andersson, K. Gas-Phase Chemistry of the NO-SO₂-ClO₂ System Applied

- to Flue Gas Cleaning. *Ind. Eng. Chem. Res.* **2018**, *57* (43), 14347–14354.
- (15) Liu, Y.; Pan, J.; Wang, Q. Removal of Hg⁰ from Containing-SO₂/NO Flue Gas by Ultraviolet/H₂O₂ Process in a Novel Photochemical Reactor. *AIChE J.* **2014**, *60* (6), 2275–2285.
- (16) Liu, Y.; Wang, Y.; Liu, Z.; Wang, Q. Oxidation Removal of Nitric Oxide from Flue Gas Using UV Photolysis of Aqueous Hypochlorite. *Environ. Sci. Technol.* **2017**, *51* (20), 11950–11959.
- (17) Wang, Z.; Lun, L.; Tan, Z.; Zhang, Y.; Li, Q. Simultaneous Wet Desulfurization and Denitration by an Oxidant Absorbent of NaClO₂/CaO₂. *Environ. Sci. Pollut. Res.* **2019**, *26* (28), 29032–29040.
- (18) Jin, D. S.; Deshwal, B. R.; Park, Y. S.; Lee, H. K. Simultaneous Removal of SO₂ and NO by Wet Scrubbing Using Aqueous Chlorine Dioxide Solution. *J. Hazard. Mater.* **2006**, *135* (1–3), 412–417.
- (19) Deshwal, B. R.; Jin, D. S.; Lee, S. H.; Moon, S. H.; Jung, J. H.; Lee, H. K. Removal of NO from Flue Gas by Aqueous Chlorine-Dioxide Scrubbing Solution in a Lab-Scale Bubbling Reactor. *J. Hazard. Mater.* **2008**, *150* (3), 649–655.
- (20) White, V.; Torrente-Murciano, L.; Sturgeon, D.; Chadwick, D. Purification of Oxyfuel-Derived CO₂. *Int. J. Greenh. Gas Control* **2010**, *4* (2), 137–142.
- (21) Torrente-Murciano, L.; White, V.; Petrocelli, F.; Chadwick, D. Sour Compression Process for the Removal of SO_x and NO_x from Oxyfuel-Derived CO₂. *10th Int. Conf. Greenh. Gas Control Technol.* **2011**, *4*, 908–916.
- (22) Liemans, I.; Alban, B.; Tranier, J. P.; Thomas, D. SO_x and NO_x Absorption Based Removal into Acidic Conditions for the Flue Gas Treatment in Oxy-Fuel Combustion. *10th Int. Conf. Greenh. Gas Control Technol.* **2011**, *4*, 2847–2854.
- (23) Trainer, J. P.; Court, P.; Darde, A.; Perrin, N. CO₂ Purification Unit for Oxy-Coal Combustion Systems. *1st International Oxyfuel Combustion Conference Cottbus*. Germany 2009.
- (24) Shah, M.; Degenstein, N.; Zafir, M.; Kumar, R.; Bugayong, J.; Burgers, K. Near Zero Emissions Oxy-Combustion CO₂ Purification Technology. *10th Int. Conf. Greenh. Gas Control Technol.* **2011**, *4*, 988–995.
- (25) Stokie, D.; Verma, P.; Kumfer, B. M.; Yablonsky, G.; Suresh, A. K.; Axelbaum, R. L. Pilot-Scale Testing of Direct Contact Cooler for the Removal of SO_x and NO_x from the Flue Gas of Pressurized Oxy-Coal Combustion. *Chem. Eng. J.* **2021**, *414*, 128757.
- (26) White, V.; Wright, A.; Tappe, S.; Yan, J. The Air Products Vattenfall Oxyfuel CO₂ Compression and Purification Pilot Plant at Schwarze Pumpe. *Energy*

Procedia **2013**, 37, 1490–1499.

- (27) Johansson, J.; Normann, F.; Sarajlic, N.; Andersson, K. Technical-Scale Evaluation of Scrubber-Based, Co-Removal of NO_x and SO_x Species from Flue Gases via Gas-Phase Oxidation. *Ind. Eng. Chem. Res.* **2019**, 58 (48), 21904–21912.
- (28) Shen, C. H.; Rochelle, G. T. Nitrogen Dioxide Absorption and Sulfite Oxidation in Aqueous Sulfite. *Environ. Sci. Technol.* **1998**, 32 (13), 1994–2003.
- (29) Senjo, T.; Kobayashi, M. Process for Removing Nitrogen Oxides from Gas. Google Patents 1976.
- (30) Littlejohn, D.; Chang, S. G. Removal of Nox and So2 from Flue-Gas by Peracid Solutions. *Ind. Eng. Chem. Res.* **1990**, 29 (7), 1420–1424.
- (31) Adewuyi, Y. G.; He, X. D.; Shaw, H.; Lolertpihop, W. Simultaneous Absorption and Oxidation of NO and SO₂ by Aqueous Solutions of Sodium Chlorite. *Chem. Eng. Commun.* **1999**, 174, 21–51.
- (32) Chien, T. W.; Chu, H. Removal of SO₂ and NO from Flue Gas by Wet Scrubbing Using an Aqueous NaClO₂ Solution. *J. Hazard. Mater.* **2000**, 80 (1–3), 43–57.
- (33) Sun, C. L.; Zhao, N.; Wang, H. Q.; Wu, Z. B. Simultaneous Absorption of NO_x and SO₂ Using Magnesia Slurry Combined with Ozone Oxidation. *Energy & Fuels* **2015**, 29 (5), 3276–3283.
- (34) Sun, Y.; Hong, X. W.; Zhu, T. L.; Guo, X. Y.; Xie, D. Y. The Chemical Behaviors of Nitrogen Dioxide Absorption in Sulfite Solution. *Appl. Sci.* **2017**, 7 (4).
- (35) Kang, M. S.; Shin, J.; Yu, T. U.; Hwang, J. Simultaneous Removal of Gaseous NO_x and SO₂ by Gas-Phase Oxidation with Ozone and Wet Scrubbing with Sodium Hydroxide. *Chem. Eng. J.* **2020**, 381.
- (36) Zhang, J.; Zhang, R.; Chen, X.; Tong, M.; Kang, W.; Guo, S.; Zhou, Y.; Lu, J. Simultaneous Removal of NO and SO₂ from Flue Gas by Ozone Oxidation and NaOH Absorption. *Ind. Eng. Chem. Res.* **2014**, 53 (15), 6450–6456.
- (37) Selinger, J. *Pilot Plant NO₂ Removal with Aqueous Solutions of Sodium Sulfite*; Austin, 2017.
- (38) Hutson, N. D.; Krzyzyska, R.; Srivastava, R. K. Simultaneous Removal of SO₂, NO_x, and Hg from Coal Flue Gas Using a NaClO₂-Enhanced Wet Scrubber. *Ind. Eng. Chem. Res.* **2008**, 47 (16), 5825–5831.
- (39) Sun, W. Y.; Ding, S. L.; Zeng, S. S.; Su, S. J.; Jiang, W. J. Simultaneous Absorption of NO_x and SO₂ from Flue Gas with Pyrolusite Slurry Combined

- with Gas-Phase Oxidation of NO Using Ozone. *J. Hazard. Mater.* **2011**, *192* (1), 124–130.
- (40) Ma, Q.; Wang, Z.; Lin, F.; Kuang, M.; Whiddon, R.; He, Y.; Liu, J. Characteristics of O₃ Oxidation for Simultaneous Desulfurization and Denitration with Limestone-Gypsum Wet Scrubbing: Application in a Carbon Black Drying Kiln Furnace. *Energy and Fuels* **2016**, *30* (3), 2302–2308.
- (41) Beilke, S.; Lamb, D.; Muller, J.; Müller, J. On the Uncatalyzed Oxidation of Atmospheric SO₂ by Oxygen in Aqueous Systems. *Atmos. Environ.* **1975**, *9* (12), 1083–1090.
- (42) Larson, T. V.; Horike, N. R.; Harrison, H. Oxidation of Sulfur-Dioxide by Oxygen and Ozone in Aqueous-Solution - Kinetic Study with Significance to Atmospheric Rate Processes. *Atmos. Environ.* **1978**, *12* (8), 1597–1611.
- (43) Connick, R. E.; Zhang, Y. X.; Lee, S. Y.; Adamic, R.; Chieng, P. Kinetics and Mechanism of the Oxidation of HSO₃⁻ by O₂. 1. The Uncatalyzed Reaction. *Inorg. Chem.* **1995**, *34* (18), 4543–4553.
- (44) Mo, J. S.; Wu, Z. B.; Cheng, C. J.; Guan, B. H.; Zhao, W. R. Oxidation Inhibition of Sulfite in Dual Alkali Flue Gas Desulfurization System. *J. Env. Sci* **2007**, *19* (2), 226–231.
- (45) Littlejohn, D.; Wang, Y.; Chang, S. G. Oxidation of Aqueous Sulfite Ion by Nitrogen Dioxide. *Environ. Sci. Technol.* **1993**, *27* (10), 2162–2167.
- (46) Sapkota, V. N. A.; Fine, N. A.; Rochelle, G. T. NO₂-Catalyzed Sulfite Oxidation. *Ind. Eng. Chem. Res.* **2015**, *54* (17), 4815–4822.
- (47) Atkinson, R.; Baulch, D. L.; Cox, R. A.; Hampson, R. F.; Kerr, J. A.; Rossi, M. J.; Troe, J. Evaluated Kinetic, Photochemical and Heterogeneous Data for Atmospheric Chemistry .5. IUPAC Subcommittee on Gas Kinetic Data Evaluation for Atmospheric Chemistry. *J. Phys. Chem. Ref. Data* **1997**, *26* (3), 521–1011.
- (48) Atkinson, R.; Baulch, D. L.; Cox, R. A.; Hampson, R. F.; Kerr, J. A.; Rossi, M. J.; Troe, J. Evaluated Kinetic and Photochemical Data for Atmospheric Chemistry: Supplement VIII, Halogen Species - IUPAC Subcommittee on Gas Kinetic Data Evaluation for Atmospheric Chemistry. *J. Phys. Chem. Ref. Data* **2000**, *29* (2), 167–266.
- (49) Demore, W. B.; Sander, S. P.; Golden, D. M.; Hampson, R. F.; Kurylo, M. J.; Howard, C. J.; Ravishankara, A. R.; Kolb, C. E.; Molina, M. J.; NASA. *Chemical Kinetics and Photochemical Data for Use in Stratospheric Modeling*; Jet Propulsion Laboratory, 1997.
- (50) Watson, R. T. Rate Constants for Reactions of ClO_x of Atmospheric Interest. *J. Phys. Chem. Ref. Data* **1977**, *6* (3), 871–917.

- (51) Beyad, Y.; Burns, R.; Puxty, G.; Maeder, M. A Speciation Study of Sulfur(IV) in Aqueous Solution. *Dalt. Trans.* **2014**, 43 (5), 2147–2152.
- (52) Siddiqi, M. A.; Krissmann, J.; PetersGerth, P.; Luckas, M.; Lucas, K. Spectrophotometric Measurement of the Vapour-Liquid Equilibria of (Sulphur Dioxide plus Water). *J. Chem. Thermodyn.* **1996**, 28 (7), 685–700.
- (53) Voegelé, A. E.; Tautermann, C. S.; Loerting, T.; Hallbrucker, A.; Mayer, E.; Liedl, K. R. About the Stability of Sulfurous Acid (H₂SO₃) and Its Dimer. *Chem. Eur. J.* **2002**, 8 (24), 5644–5651.
- (54) Rhee, J. S.; Dasgupta, P. K. The Second Dissociation Constant of Sulfur Dioxide-Water. *J. Phys. Chem.* **1985**, 89 (9), 1799–1804.
- (55) Schwartz, S. E. Equilibria in the Nitrogen-Oxide Nitrogen Oxyacid-Water System. *Abstr. Pap. Am. Chem. Soc.* **1980**, 180 (Aug), 221-Phys.
- (56) Lee, Y. N.; Schwartz, S. E. Reaction-Kinetics of Nitrogen-Dioxide with Liquid Water at Low Partial-Pressure. *J. Phys. Chem.* **1981**, 85 (7), 840–848.
- (57) Park, J. Y.; Lee, Y. N. Solubility and Decomposition Kinetics of Nitrous-Acid in Aqueous-Solution. *J. Phys. Chem.* **1988**, 92 (22), 6294–6302.
- (58) Clifton, C. L.; Altstein, N.; Huie, R. E. Rate-Constant for the Reaction of NO₂ with Sulfur(IV) over the pH Range 5.3-13. *Environ. Sci. Technol.* **1988**, 22 (5), 586–589.
- (59) Zhuang, Z.; Sun, C.; Zhao, N.; Wang, H.; Wu, Z. Numerical Simulation of NO₂ Absorption Using Sodium Sulfite in a Spray Tower. *J. Chem. Technol. Biotechnol.* **2016**, 91 (4), 994–1003.
- (60) Nash, T. The Effect of Nitrogen Dioxide and of Some Transition Metals on the Oxidation of Dilute Bisulphite Solutions. *Atmos. Environ.* **1979**, 13 (8), 1149–1154.

